

A Search for Sidereal Anisotropies with Underground Muons and an All-Sky Survey for Muon Point Sources with the MACRO Detector

Search for Astrophysical Point Sources of Muons with the MACRO Detector

Arrival Time Distributions of Very High Energy Cosmic Ray Muons in MACRO

Measurement of the Muons Decoherence Function with the MACRO Experiment at Gran Sasso

Study of the Primary Cosmic Ray Composition with the MACRO Experiment at Gran Sasso

A Search for Prompt Muons using the MACRO Detector at Gran Sasso

Search for Nuclearites with the MACRO Detector

Stellar Gravitational Collapse Detection by MACRO: Characteristics and Results

LNGS - 91/08
October 1991

LNGS - 91/09
October 1991

LNGS - 91/10
October 1991

LNGS - 91/11
October 1991

LNGS - 91/12
October 1991

LNGS - 91/13
October 1991

LNGS - 91/14
October 1991

LNGS - 91/15
October 1991

受入

91-12-202
高工研四書室

受入

91-12-203
高工研四書室

受入

91-12-204
高工研四書室

受入

91-12-208
高工研四書室



CONTRIBUTIONS TO THE 22nd ICRC
The MACRO Collaboration

INFN - Laboratori Nazionali del Gran Sasso

A Search for Sidereal Anisotropies with Underground Muons and an All-Sky Survey for Muon Point Sources with the MACRO Detector

The MACRO Collaboration

Bari: R. Bellotti, F. Cafagna, M. Calicchio, G. De Cataldo, C. De Marzo, O. Erriquez, C. Favuzzi, P. Fusco, N. Giglietto, P. Spinelli; **Bartol:** J. Petrakis; **Bologna:** S. Cecchini, G. Giacomelli, G. Mandrioli, A. Margiotta-Neri, P. Matteuzzi, L. Patrizii, F. Predieri, G.L. Sanzani, E. Scaparoni, P. Serra Lugaresi, M. Spurio, V. Togo; **Boston:** S. Ahlen, R. Cormack, E. Kearns, S. Klein, G. Ludlam, A. Marin, C. Okada, J. Stone, L. Sulak, W. Worstell; **Caltech:** B. Barish, S. Coutu, J. Hong, E. Katsuvounidis, S. Kyriazopoulou, G. Liu, R. Liu, D. Michael, C. Peck, N. Pignatano, K. Scholberg, J. Steele, C. Walter; **Drexel:** C. Lane, R. Steinberg; **Frascati:** G. Battistoni, H. Bilokon, C. Bloise, P. Campana, P. Cavallo, V. Chiarella, C. Forti, A. Grillo, E. Iarocci, A. Marini, V. Patera, F. Ronga, L. Satta, M. Spinetti, V. Valente; **Gran Sasso:** C. Gustavino, J. Reynoldson; **Indiana:** A. Habig, R. Heinz, L. Miller, S. Mufson, J. Musser, S. Nutter; **L'Aquila:** A. Di Credico, P. Monacelli; **Lecce:** P. Bernardini, G. Mancarella, D. Martello, O. Palamara, S. Petrera, P. Pistilli, A. Surdo; **Michigan:** E. Diehl, D. Levin, M. Longo, C. Smith, G. Tarlé; **Napoli:** M. Ambrosio, G. C. Barbarino, F. Guarino, G. Osteria; **Pisa:** A. Baldini, C. Bemporad, F. Cei, G. Giannini, M. Grassi, R. Pazzi; **Roma:** G. Auriemma, S. Bussino, C. Chiera, P. Chrysicopoulou, A. Corona, M. DeVincenzi, L. Foti, E. Lamanna, P. Lipari, G. Martellotti, G. Rosa, A. Sciubba, M. Severi; **Sandia Labs:** P. Green; **Texas A&M:** R. Webb; **Torino:** V. Bisi, P. Giubellino, A. Marzari Chiesa, M. Maserà, M. Monteno, S. Parlati, L. Ramello, M. Sitta

*Univ. di Trieste

**Univ. della Basilicata

INTRODUCTION

Ultrahigh energy muons can be used to search for point sources of cosmic rays. Muons produced in the Earth's atmosphere preserve the directionality of the source for energetic neutral primaries. We report here an analysis of 1.7 million muons seen by the MACRO detector in which we search the sky for sources of excess cosmic ray flux. Observation of such sources may reveal the nature of the source and/or the mediating particle. Additionally, a search for large-scale anisotropies in the sidereal distributions of event arrivals is reported.

DATA SELECTION

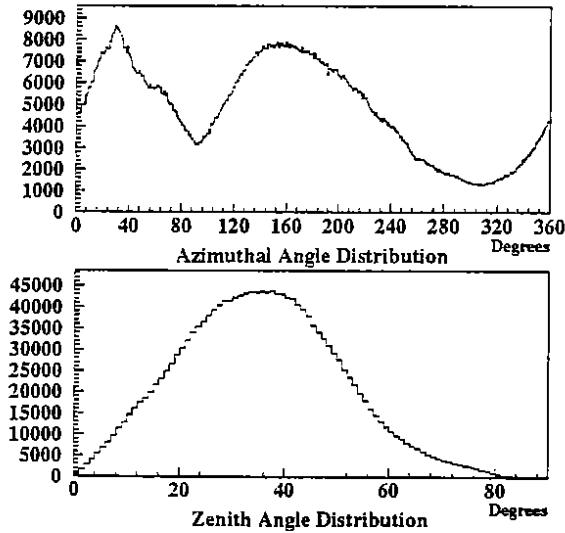
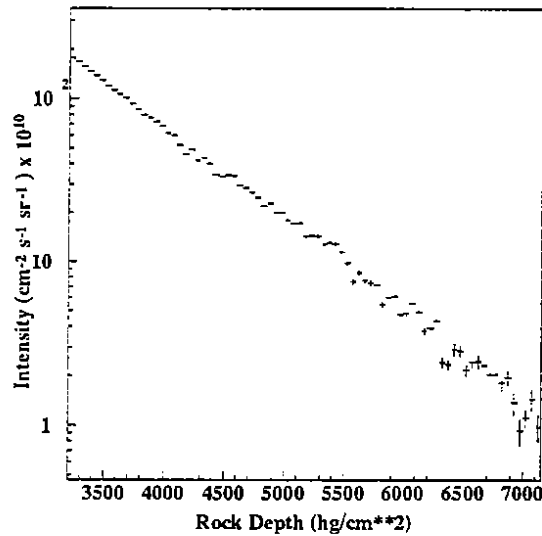
The muon data reported here were collected by the first MACRO supermodule (12 m \times 12 m \times 4.8 m) during two data runs, and by the first and second MACRO supermodules (24 m \times 12 m \times 4.8 m) during a third data run. The dates, the live times, the number of μ triggers, and the number of muons analyzed for these three data samples are given in Table 1.

In the present study, single muons with successfully reconstructed tracks were retained if they crossed at least 4 out of 10 streamer tube planes. For isotropic events satisfying this criterion, the first MACRO supermodule has an acceptance of $S\Omega \sim 800 \text{ m}^2 \text{ sr}$; the first and second MACRO supermodules have $S\Omega \sim 1,600 \text{ m}^2 \text{ sr}$. For this study, we have excluded data-taking periods in which the event rate fluctuated by $\gtrsim 2\sigma$ from the mean event rate for the entire run. Individual source fluctuations would not affect rates in this way. In addition, we have excluded particularly noisy events that are typically the result of muon interactions in the apparatus. A total of approximately 1.7×10^6 muons survive these cuts.

Table 1. Run Parameters for Three Data Samples

Run Period	Supermodules Operational	Live time (hours)	No. of μ Triggers	No. of μ Analyzed
Feb 27, 1989–May 30, 1989	1	1881.14	243,640	223,940
Nov 11, 1989–May 10, 1990	1	2909.37	356,289	319,275
May 10, 1990–Feb 5, 1991	1,2	5032.82	1,378,937	1,185,792

The zenith angle and azimuthal angle distributions for all the events in the local reference frame are shown in Figure 1. To verify our data analysis procedures, we calculated the muon intensity as a function of rock depth for events with zenith angle $\theta \leq 60^\circ$; this cut is relevant only to the depth-intensity relationship¹ and has not been used in the subsequent analysis. For each data sample the events were divided into bins of equal solid angle $\Delta\Omega$ ($\Delta\phi = 3.0^\circ$, $\Delta\cos\theta = 0.04$). For the three data samples, intensities corrected to the vertical were computed for each solid angle bin using the appropriate value of the detector acceptance. These intensities were then combined into bins of rock thickness of width 50 hg/cm² using an elevation map of the Gran Sasso mountain². The intensities at each rock thickness were combined by weighting every contribution according to its uncertainty. The vertical intensity as a function of rock thickness for muons with $\theta \leq 60^\circ$ is shown in Figure 2.

**Figure 1.** Azimuthal and zenith angle distributions.**Figure 2.** Intensity distribution for the complete data sample.

SIDEREAL ANISOTROPIES

In Figure 3 are shown the right ascension and declination distributions for the

events in the three data samples. The expected right ascension and declination distributions have been calculated by Monte Carlo simulation. Event positions were chosen from the observed two-dimensional distribution of zenith and azimuthal angles. Arrival times were simulated on a run-by-run basis by a Poisson process. For each run the observed event rate was used as the mean. All dead-time gaps were explicitly taken into account. Right ascensions and declinations were computed and analyzed in the same way as the real events. This procedure was repeated 25 times. In Figure 3, the average right ascension and declination distributions generated in this manner are shown as dotted lines. The Kolmogorov-Smirnov test yields a probability of 0.999 that the simulated distributions and the data distributions are drawn from the same parent population.

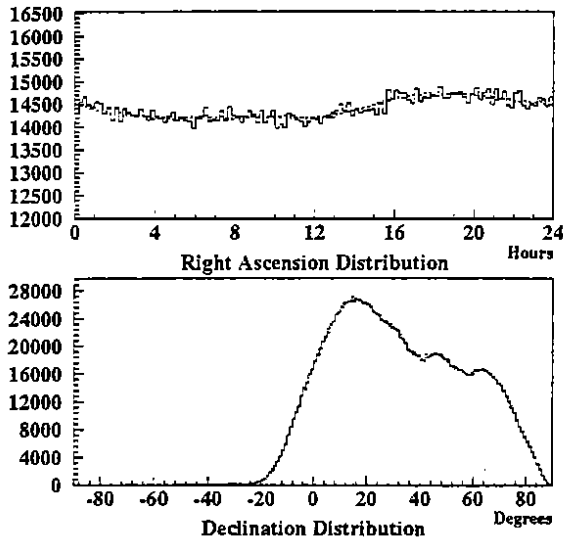


Figure 3. Right ascension and declination distributions. Monte Carlo backgrounds are super-imposed.

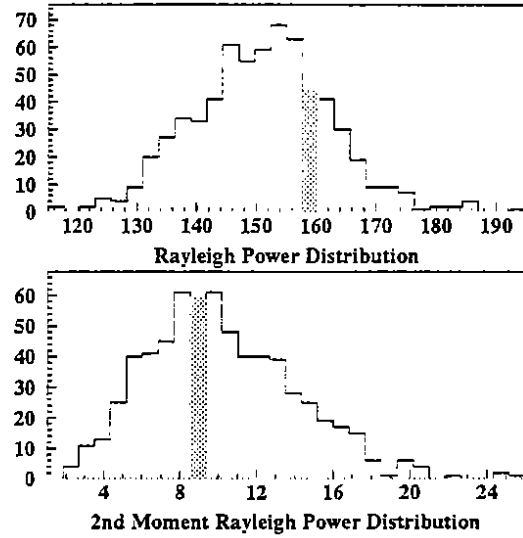


Figure 4. Rayleigh power distributions for the first and second moments. Data values are in shaded bins.

We have searched for sidereal anisotropies in the right ascension distribution using the Rayleigh test. The Rayleigh power of the right ascension distribution is given by $n\bar{R}^2 = \frac{1}{n} \left\{ \left[\sum_{i=1}^n \cos(2\pi m \alpha_i / 24) \right]^2 + \left[\sum_{i=1}^n \sin(2\pi m \alpha_i / 24) \right]^2 \right\}$, where α_i is the right ascension of the i^{th} event, n is the total number of muons, and $m = (1, 2)$ for the first/second moment, respectively.

Since event times in our simulations are chosen from a Poisson distribution, the simulations will not exhibit sidereal anisotropies. We have computed the expected distributions for the first and second moments of the Rayleigh power that reflect the live time distribution from 652 Monte Carlo simulations. Figure 4 shows these distributions. Values for the two moments computed from the MACRO data distributions fall in the shaded bins. The data samples we have investigated are consistent with a right ascension distribution with no sidereal anisotropies.

ALL-SKY SURVEY

Using our Monte Carlo distributions we can make an all-sky search for point sources of muons in excess of the expected background. First the data were binned in equal solid angle bins $\Delta\Omega$ ($\Delta\alpha = 3.0^\circ$, $\Delta\sin\delta = 0.04$). An average of 25 Monte Carlo data runs was then used as the expected background. These background events were binned in the same way as the data.

We computed the deviation from the mean for every bin, $\delta = (n - e)/\sqrt{e}$, where n is the number of events in the bin and e is the expected background. In Figure 5 we show the distribution of these deviations. There are no deviations greater than 3.8σ . Superimposed onto this distribution is the best-fitting Gaussian $\chi^2/\text{DoF} = 85/100$. The mean of this Gaussian is 1.4×10^{-3} and the rms is 1.01, as is expected from a random distribution.

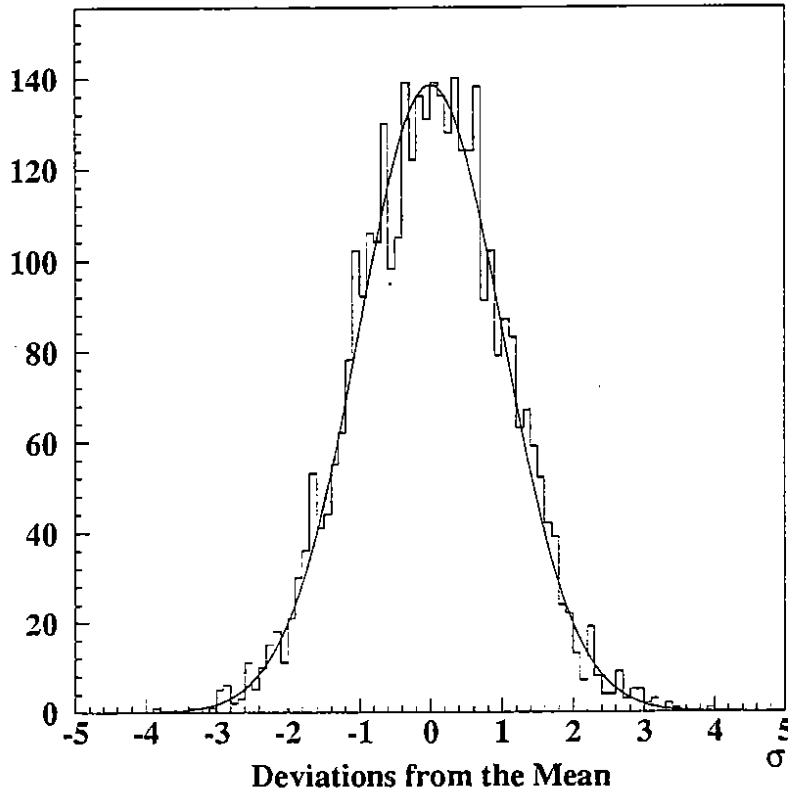


Figure 5. Distribution of deviations from the mean in the all-sky survey.

REFERENCES

1. T.K. Gaisser, *Cosmic Rays and Particle Physics*, Cambridge University Press, 34 (1990).
2. The MACRO Collaboration, *Phys. Lett. B* **249**, 149 (1990).

Search for Astrophysical Point Sources of Muons with the MACRO Detector

The MACRO Collaboration

Bari: R. Bellotti, F. Cafagna, M. Calicchio, G. De Cataldo, C. De Marzo, O. Enriquez, C. Favuzzi, P. Fusco, N. Giglietto, P. Spinelli; **Bartol:** J. Petrakis; **Bologna:** S. Cecchini, G. Giacomelli, G. Mandrioli, A. Margiotta-Neri, P. Matteuzzi, L. Patrizii, F. Predieri, G.L. Sanzani, E. Scapparone, P. Serra Lugaresi, M. Spurio, V. Togo; **Boston:** S. Ahlen, R. Cormack, E. Kearns, S. Klein, G. Ludlam, A. Marin, C. Okada, J. Stone, L. Sulak, W. Worstell; **Caltech:** B. Barish, S. Coutu, J. Hong, E. Katsivounidis, S. Kyriazopoulou, G. Liu, R. Liu, D. Michael, C. Peck, N. Pignatano, K. Scholberg, J. Steele, C. Walter; **Drexel:** C. Lane, R. Steinberg; **Frascati:** G. Battistoni, H. Bilokon, C. Bloise, P. Campana, P. Cavallo, V. Chiarella, C. Forti, A. Grillo, E. Iarocci, A. Marini, V. Patera, F. Ronga, L. Satta, M. Spinetti, V. Valente; **Gran Sasso:** C. Gustavino, J. Reynoldson; **Indiana:** A. Habig, R. Heinz, L. Miller, S. Mufson, J. Musser, S. Nutter; **L'Aquila:** A. Di Credico, P. Monacelli; **Lecce:** P. Bernardini, G. Mancarella, D. Martello, O. Palamara, S. Petrera, P. Pistilli, A. Surdo; **Michigan:** E. Diehl, D. Levin, M. Longo, C. Smith, G. Tarlé; **Napoli:** M. Ambrosio, G. C. Barbarino, F. Guarino, G. Osteria; **Pisa:** A. Baldini, C. Bemporad, F. Cei, G. Giannini, M. Grassi, R. Pazzi; **Roma:** G. Auriemma, S. Bussino, C. Chiera, P. Chrysicopoulou, A. Corona, M. DeVincenzi, L. Foti, E. Lamanna, P. Lipari, G. Martellotti, G. Rosa, A. Sciubba, M. Severi; **Sandia Labs:** P. Green; **Texas A&M:** R. Webb; **Torino:** V. Bisi, P. Giubellino, A. Marzari Chiesa, M. Masera, M. Monteno, S. Parlati, L. Ramello, M. Sitta

*Univ. di Trieste

**Univ. della Basilicata

Due to its high tracking resolution, MACRO is well suited to search for muon excesses in the direction of celestial point sources of VHE or UHE photons. In this paper we analyze the muons from the direction of the reported sources of VHE and UHE photons: Cyg X3, Her X1, 1E2259+59 and the Crab.

THE MACRO EXPERIMENT

Since MACRO has been described in detail elsewhere,¹ we describe here only its characteristics relevant to muon astronomy. The instrumental angular resolution of the limited streamer tube system that provides the tracking information is nominally 0.2° for tracks traversing the entire apparatus; the resolution degrades for shorter tracks. After folding in the effect of multiple Coulomb scattering in the rock, the overall angular resolution is $\approx 0.8^\circ$. This value is consistent with the measured relative angular spread of muons in multimMuon events.

Muons reaching the apparatus traverse an average pathlength of 3800 meters of water equivalent (MWE) and a minimum pathlength of 3100 MWE. The threshold energy for single muons is ≈ 1.5 TeV.

DATA SELECTION AND ANALYSIS

The data analyzed consist of 3 data samples² which total approximately 1.7×10^6 muons obtained over a live-time Δt of 9823 hours. We have selected for this analysis single muon events that cross at least 4 of 10 horizontal streamer tube planes.

Steady Muon Signals: We have searched for an excess of muon tracks pointing back to a 1.5° half-angle cone centered on Cyg X3, Her X1, 1E2259+59 and the Crab. The average pathlength traversed by muons from each source window and the number of events, n , in each window are listed in Table 1. The expected number of background counts determined by Monte Carlo simulation, n_{bkd} , is also given in Table 1. These Monte Carlo simulations explicitly account for the detector live-time distribution throughout the data taking periods. There is no evident signal from any source at the 1σ level.

The upper limit to the steady muon flux at the 90% C.L. was computed by $F_{\text{stdy}} = 1.28\sqrt{n_{\text{bkd}}}/(\bar{\epsilon}A_{\text{eff}}f\Delta t)$, where $\bar{\epsilon} = 0.87$ is an estimate of the live-time weighted efficiency; A_{eff} is the live-time weighted effective area for the window; and f is the fractional time the source window is $\geq 10^\circ$ above the horizon. The values for A_{eff} , f , and F_{stdy} are given in Table 1.

Table 1. Search for Steady Muon Signals from Point Sources

Source	<depth> (MWE)	n	n_{bkd}	A_{eff} (m^2)	f	F_{stdy} ($\text{cm}^{-2}\text{s}^{-1}$)
Cyg X3	3960	491	485	190	.66	$< 7.4 \times 10^{-13}$
Her X1	3885	455	489	194	.64	$< 7.5 \times 10^{-13}$
1E2259+59	3795	584	608	183	1.0	$< 5.7 \times 10^{-13}$
Crab	3560	520	523	200	.52	$< 9.3 \times 10^{-13}$

Periodic Muon Signals: In the search for periodic muon signals in a 1.5° half-angle cone, a correction was applied to the arrival time of each event to account for the earth's motion with respect to the solar system barycenter.

For Cyg X3, we searched for a muon signal modulated by the 4.8 hr X-ray period using the parabolic ephemeris of van der Klis and Bonnet-Bidaud.³ The phase diagram for these data are shown in Figure 1 as a solid line and the average background is shown as a dotted line. This figure shows that the largest deviation above background is at the 2σ level.

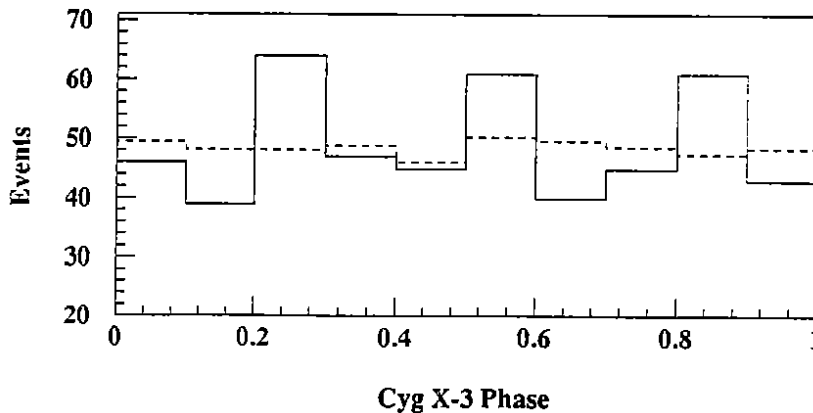


Figure 1. Phase diagram for Cyg X3 in a 1.5° half-angle cone.

For Her X1, we searched for a muon signal which was modulated by either the 1.7^d orbital period⁴ or the 35^d (presumed precessional) period.⁵ For the 1E2259+59 data, we searched for a muon signal modulated by the first and second harmonic of the 6.98^s pulsar period.⁶ (A large fraction of the X-ray power is emitted in the second harmonic.) For 1E2259+59 the X-ray period has been determined accurately enough to maintain phase coherence only over ≈ 30 days. We therefore broke the data into 17 separate 30^d segments, analyzing each segment individually. We searched for evidence of a statistically significant modulated signal in these three sources using both the Rayleigh and Protheroe tests. In Table 2 we list for Cyg X3 and Her X1 the probabilities, $W(> n\bar{R}^2)$ and $W(> \Upsilon_n)$, that the Rayleigh power, $n\bar{R}^2$, and the Protheroe power, Υ_n , have values at least as large as we found for events distributed uniformly in phase—a test of the null hypothesis. These probabilities were computed by Monte Carlo simulation. Both tests imply there are no statistically significant modulated muon signals at the periods investigated. There is also no evidence in 1E2259+59 for a muon signal modulated with the pulsar period. In Table 2 we have estimated the upper limit to the modulated flux in the 1.5° half-angle cone from the relation $F_{\text{mod}} = (n - n_{\text{bkd}} + 1.28\sqrt{n})/(\bar{\epsilon}A_{\text{eff}}\Delta t)$, using the phase bin with the largest excess above background. For 1E2259+59 a similar calculation yields $F_{\text{mod}} \lesssim 2 \times 10^{-12} \text{ cm}^{-2} \text{ s}^{-1}$ as a typical value for an individual 30 day run.

Table 2. Search for a Modulated Muon Signal from Point Sources

Source	P_0	$W(> n\bar{R}^2)$	$W(> \Upsilon_n)$	$F_{\text{mod}} (\text{cm}^{-2} \text{s}^{-1})$
Cyg X3	4.8^h	0.90	0.52	$< 6.9 \times 10^{-13}$
Her X1	1.70^d	0.52	0.68	$< 4.1 \times 10^{-13}$
Her X1	34.9^d	0.64	0.32	$< 6.8 \times 10^{-13}$

In Figure 2 we present our flux limit from the direction of Cyg X3, compared with the limits from other underground detectors.

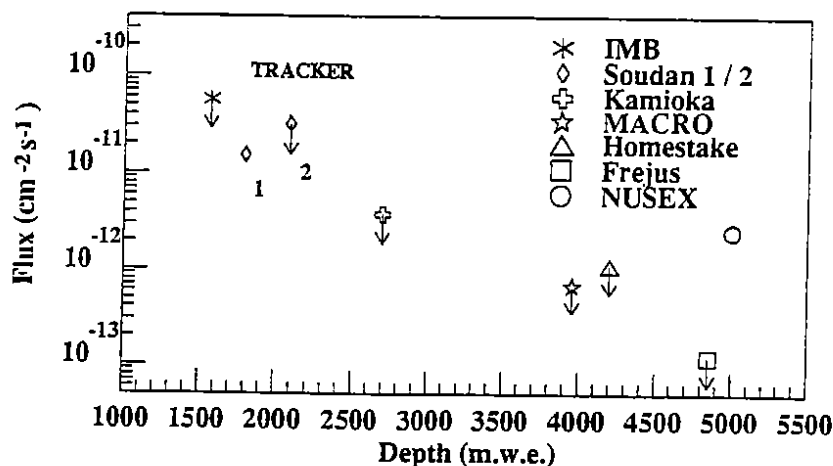


Figure 2. Measurements of the modulated muon flux from Cyg X3.

Period Search: We have searched through period space for a modulated muon signal with a period displaced from the fiducial periods P_0 . We chose for the

increment in period space 10% of an Independent Fourier Spacing (IFS), $\Delta P = 0.1P_0^2/T$. For Cyg X3 and Her X1, T is the run time for a data sample.² For 1E2259+59, T is equal to 30 days. We have searched through 30 IFS on either side of P_0 .

Let χ_{\max} represent the maximum Rayleigh or Protheroe power we have found for any source in our period search. As a test of the null hypothesis, we have calculated the probability W that χ_{\max} represents a random fluctuation in the rate of cosmic ray muons, $W(> \chi_{\max}) = 1 - (1 - p_1)^N$. In this expression, p_1 is the probability of obtaining χ_{\max} from events distributed randomly in phase as determined by Monte Carlo simulation, and N is the effective number of trials. For Cyg X3 and Her X1, $N \approx 61 \times 3 \times 3$ - we have searched through 61 IFS; 3 represents the penalty for oversampling the IFS⁷; and 3 is the number of run periods searched. For 1E2259+59, $N \approx 61 \times 3 \times 17$. In all cases investigated, $W(> \chi_{\max}) \gg 0.99$, which suggests that there is no modulated muon signal with a period displaced slightly from P_0 .

Search for Short Term Variability in Cyg X3: The muon events from the 1.5° half-angle cone around Cyg X3 for data sample 3 have been analyzed for short term variability on a time scale of one day. During this period there were three reported radio outbursts, a large burst on 21 January 1991 and two lesser flares on 14 August and 5 October 1990.⁸

The points in Figure 3 show the deviations ($n - e$) for every day during this period, where n is the number of events in the window and e is the expected number of events on that day determined by Monte Carlo simulation. We have found no deviations in excess of 3.9σ . In periods consisting of five days on either side of the radio bursts, no deviations above 3σ were found. The solid curve in Figure 3 shows the predictions of Poisson statistics. Clearly the simulated distribution matches the data distribution well, reinforcing the conclusion that MACRO saw no statistically significant outburst during the period of data sample 3.

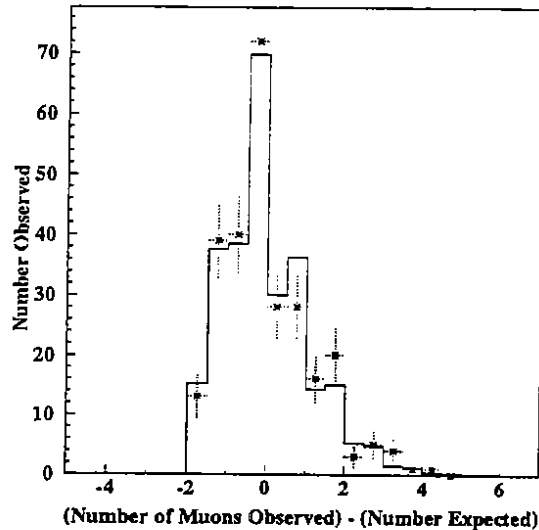


Figure 3. Daily deviations from expected for Cyg X3.

REFERENCES

1. The MACRO Collaboration, *Phys. Lett. B* **249**, 149 (1990).
2. The MACRO Collaboration, HE4.3-7, these Proceedings.
3. M. van der Klis, and J.M. Bonnet-Bidaud, *Astronomy and Astrophysics* **214**, 203 (1989).
4. J.E. Deeter, P.E. Boynton, and S.H. Pravdo, *Astrophysical Journal* **247**, 1003 (1981).
5. H. Ögelman, *Astronomy and Astrophysics* **172**, 79 (1987).
6. K. Koyama, et al., *Pub. Astron. Soc. Japan* **41**, 461 (1989).
7. O.C. de Jager, Potchefstroom University, Ph.D. dissertation (1987).
8. The Soudan 2 Collaboration, M.A. Thomson, et al., preprint (1991).

Arrival Time Distributions of Very High Energy Cosmic Ray Muons in MACRO

The MACRO Collaboration

Bari: R. Bellotti, F. Cafagna, M. Calicchio, G. De Cataldo, C. De Marzo, O. Erriquez, C. Favuzzi, P. Fusco, N. Giglietto, P. Spinelli; **Bartol:** J. Petrakis; **Bologna:** S. Cecchini, G. Giacomelli, G. Mandrioli, A. Margiotta-Neri, P. Matteuzzi, L. Patrizi, F. Predieri, G.L. Sanzani, E. Scapparone, P. Serra Lugaresi, M. Spurio, V. Togo; **Boston:** S. Ahlen, R. Cormack, E. Kearns, S. Klein, G. Ludlam, A. Marin, C. Okada, J. Stone, L. Sulak, W. Worstell; **Caltech:** B. Barish, S. Coutu, J. Hong, E. Katsivounidis, S. Kyriazopoulou, G. Liu, R. Liu, D. Michael, C. Peck, N. Pignatano, K. Scholberg, J. Steele, C. Walter; **Drexel:** C. Lane, R. Steinberg; **Frascati:** G. Battistoni, H. Bilokon, C. Bloise, P. Campana, P. Cavallo, V. Chiarella, C. Forti, A. Grillo, E. Iarocci, A. Marini, V. Patera, F. Ronga, L. Satta, M. Spinetti, V. Valente; **Gran Sasso:** C. Gustavino, J. Reynoldson; **Indiana:** A. Habig, R. Heinz, L. Miller, S. Mufson, J. Musser, S. Nutter; **L'Aquila:** A. Di Credico, P. Monacelli; **Lecce:** P. Bernardini, G. Mancarella, D. Martello, O. Palamara, S. Petrer, P. Pistilli, A. Surdo; **Michigan:** E. Diehl, D. Levin, M. Longo, C. Smith, G. Tarlé; **Napoli:** M. Ambrosio, G. C. Barbarino, F. Guarino, G. Osteria; **Pisa:** A. Baldini, C. Bemporad, F. Cei, G. Giannini, M. Grassi, R. Pazzi; **Roma:** G. Auriemma, S. Bussino, C. Chiera, P. Chrysicopoulou, A. Corona, M. DeVincenzi, L. Foti, E. Lamanna, P. Lipari, G. Martellotti, G. Rosa, A. Sciubba, M. Severi; **Sandia Labs:** P. Green; **Texas A&M:** R. Webb; **Torino:** V. Bisi, P. Giubellino, A. Marzari Chiesa, M. Maser, M. Monteno, S. Parlati, L. Ramello, M. Sitta

*Univ. di Trieste

**Univ. della Basilicata

It is generally assumed that Galactic cosmic rays have a random arrival time distribution. There may be mechanisms which introduce time modulations, as suggested by Weekes.¹ For charged primary cosmic rays the magnetic fields between the source and the earth will reduce or eliminate such modulations, with the exception of the highest energy cosmic rays. Other experiments have reported a non-random component in the arrival times of very high energy cosmic rays. Bhat et al.,² analyzing Cherenkov light pulses produced by protons with $E_p > 100$ TeV, reported a correlation at times ≤ 40 s. Badino et al.,³ using an underground detector in the Mount Blanc tunnel, reported a similar signal at times of ~ 38 s for muons with energies larger than $E_\mu \simeq 380$ GeV, originating from primaries with $E_p \geq 50$ TeV. Other experiments have not found any signal.⁴⁻¹⁰

In this paper we report a study of the time distributions of single and multiple muons detected by the streamer tube system of the first two MACRO supermodules and by the scintillators of the first supermodule(SM). About 10^6 muon events were observed in a period of about one year. The arrival time separation distributions of consecutive muons from milliseconds to several hundred seconds have been measured and analysed in terms of the random distribution function, with which they are consistent. For all events selected the time of arrival was obtained from the atomic clock. The precision of the clock is about $1 \mu\text{s}$ absolute and $0.1 \mu\text{s}$ relative.

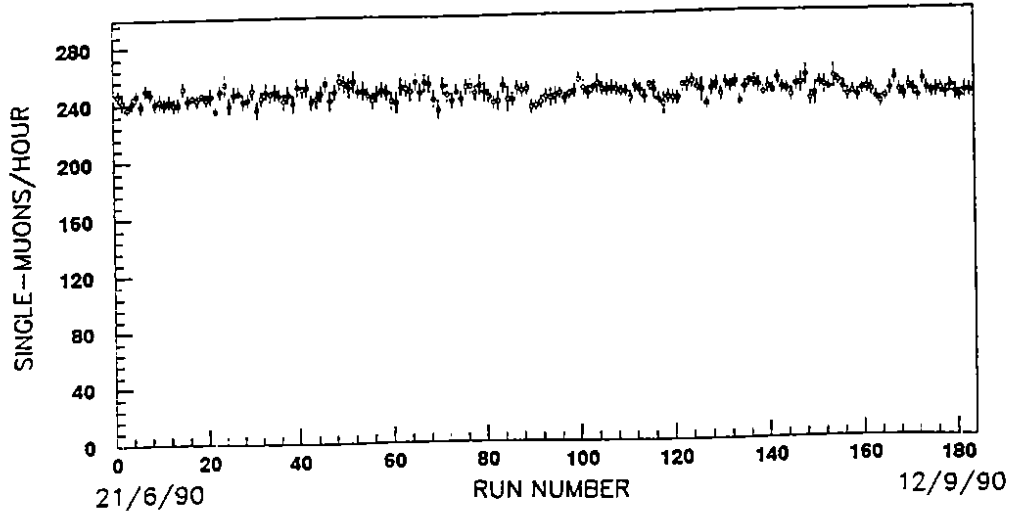


Fig. 1. The Time evolution of the number of single muons per hour.

The data were divided into four periods. We show here only the data from June 21 till September 12, 1990, taken with 2 SM. Runs which lasted less than 3 hours were not considered. The number of single muon events per hour are plotted in Fig. 1. The data fall well within the expected statistical fluctuations.

For this analysis of time correlations we study, for each muon arriving at time t_0 , the time difference of the next muon ($t_1 - t_0$) and of the following four muons, ($t_2 - t_0$), ($t_3 - t_0$), ($t_4 - t_0$) and ($t_5 - t_0$). The data were corrected for muon trigger dead times and fitted to the Gamma Function (Poissonian of order M)

$$G(t; \lambda, M) = N \frac{\lambda(\lambda t)^{M-1} e^{-\lambda t}}{(M-1)!} \quad (1)$$

where λ is the inverse of the mean value of the time difference ($t_1 - t_0$) between two consecutive muons, M is the order of the distribution and N is a normalization factor. For the ($t_1 - t_0$) fits we left $1/\lambda$ as a free parameter, using $M=1$. For $M=1$, formula (1) reduces to an exponential function

$$G(t; \lambda, 1) = N \lambda e^{-\lambda t} \quad (2)$$

The fits of the ($t_1 - t_0$) data to eq. (1) shown in Table 1 have reasonable χ^2 per Degree of Freedom (DoF). The λ coefficient should be the same for all order distributions, M , of the same period. In fact the experimental distributions of order $M \geq 2$ are well described by the gamma function of order M with parameter λ determined from the ($t_1 - t_0$) distribution (see Table 1). Direct fits of higher order distributions to Eq. 1 yield values of $1/\lambda$ equal, within errors, to that from the ($t_1 - t_0$) distribution.

Table 1. Results of the fits of M-fold time distributions for single and multiple muon events to the Gamma Function (Eq. 1). Note that the fits use data points in finer bins than those shown in the figures.

Distrib.	Fit to single muon distribution		Prob. of Kolmog. test (%)	Fit to multimMuon distribution		Prob. of Kolmog. test (%)
	$1/\lambda(s)$	χ^2/DoF		$1/\lambda(s)$	χ^2/DoF	
$(t_1 - t_0)$	14.66 ± 0.03	228/249	88.4	306 ± 3	194/199	97.8
$(t_2 - t_0)$	14.77 ± 0.03	325/346	13.8	306 ± 2	294/299	63.3
$(t_3 - t_0)$	14.73 ± 0.02	478/399	32.2	306 ± 2	280/299	86.2
$(t_4 - t_0)$	14.70 ± 0.02	495/449	49.6	305 ± 2	362/349	50.2
$(t_5 - t_0)$	14.69 ± 0.02	702/499	64.2	305 ± 2	370/399	29.0

In order to search for structure in the time arrival distributions, we have used the Kolmogorov-Smirnov test, which compares the cumulative distribution $F(x)$ of the experimental data with the expected random distribution $H(x)$. The measure of the deviation is $d = \max |F(x) - H(x)|$. In terms of this quantity, $F(x)$ agrees with $H(x, \lambda)$, where λ is taken from the data, with a probability of compatibility between the expected and the measured distributions given by P_k .

The Kolmogorov-Smirnov test for the $(t_M - t_0)$ distributions ($M = 1 - 5$) gives probabilities P_k greater than 13% for all distributions, thus confirming the agreement with the random distribution.

Fig. 2 shows the distributions of the time separation between consecutive (a) single and (b) multiple muon events. The multimMuon selection corresponds to selecting higher energy primaries. The distributions are clearly exponential, indicating the random nature of the majority of cosmic ray muon arrival times. Table 1 gives the parameter λ of equation 1 after fitting the distribution to the data. The fits have reasonable χ^2/DoF . The results of the Kolmogorov-Smirnov tests are also given in Table 1.

Fig. 3 shows the distribution $(t_2 - t_0)$ of the following consecutive muons, for single muon events in the data taking period. The data have a smooth appearance, with no indications of structures.

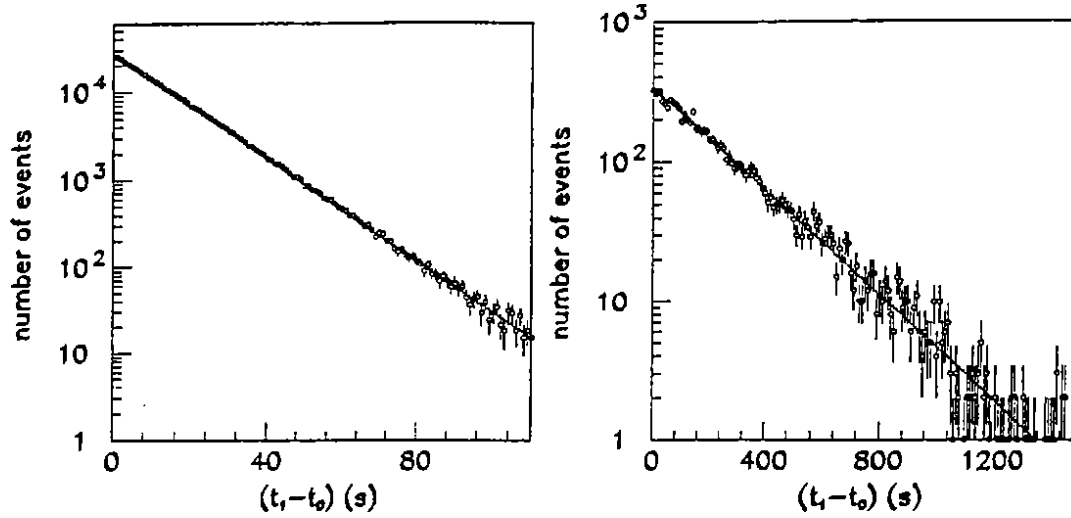


Fig. 2. Distribution of the time separation between two consecutive muon events $(t_1 - t_0)$ for (a) single and (b) multiple muons.

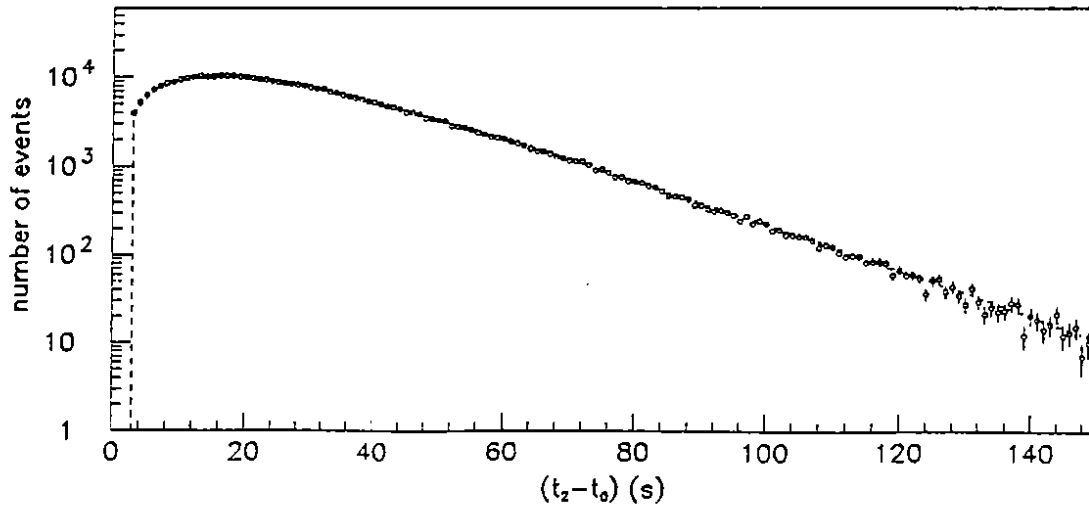


Fig. 3. The $(t_2 - t_0)$ time distribution for single muons.

In order to explore smaller time intervals we used the scintillator data from the first supermodule analyzed by the PHRASE circuits,¹¹ dedicated to searches for neutrinos from stellar collapses. The dead time of this apparatus is about 3 ms for a single scintillation counter, allowing us to explore very small time intervals with almost no dead time. Fig. 4 shows the $(t_1 - t_0)$ time distribution for single muons obtained from the scintillators of the first supermodule. No structure is seen in the time interval 10 ms–10 s. Fits of the distributions measured with the scintillators are in good agreement with those measured with the streamer tubes.

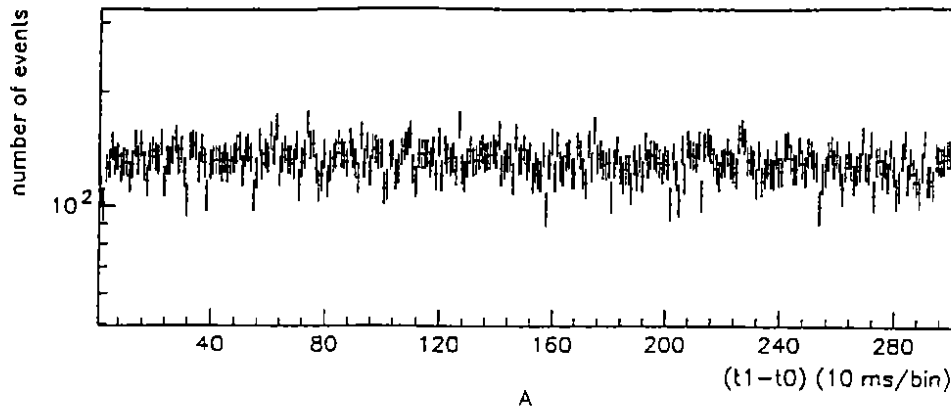


Fig. 4. The $(t_1 - t_0)$ time distribution at small time intervals for the data obtained by the scintillation counters (see text). Each bin is 10 ms wide.

In conclusion, we have presented data on the arrival time distributions of cosmic ray muons with energies larger than 1.5 TeV (at sea level). About 10^6 selected events were used; the detailed analysis of the period from June 21 till September 27, 1990 involved 407,420 muons. The muon arrival times, from milliseconds to several hundred seconds, closely follow a random distribution; there are no indications of deviations or of time anisotropies.

References

1. T. C. Weekes, *Nature* **233** 129 (1971).
2. C. L. Bhat et al., *Nature* **288**, 146 (1980).
3. G. Badino et al., *Nuovo Cimento Lett.* **28**, 93 (1980).
4. D. J. Fegan et al., in *Proc. 17th ICRC*, Paris **6**, 296 (1981).
5. S. Higashi et al., in *Proc. 16th ICRC*, Kyoto **12**, 124 (1979).
6. V. D. Ashitkov et al., in *Proc 17th ICRC*, Paris **9**, 344 (1981).
7. V. D. Ashitkov et al., in *Proc 18th ICRC*, Bangalore **7**, 129 (1983).
8. C. Morello et al., *Nuovo Cimento* **7C**, 682 (1984).
9. P. Serri, *Tesi di Laurea*, Università di Milano (1984).
10. L. Sun, *Proc. 19th ICRC*, San Diego, CA, *Papers* **2** (1985).
11. S. P. Ahlen et al., MACRO Collaboration, *Phys. Lett.* **249**, 149 (1990).
12. J. W. Elbert et al., *Phys. Rev. D* **12**, 660 (1975).
13. W. T. Eadie et al., *Stat. Meth. in Exper. Phys.*, North Holland, 269 (1971).

Measurement of the Muon Decoherence Function with the MACRO Experiment at Gran Sasso

The MACRO Collaboration

Bari: R. Bellotti, F. Cafagna, M. Calicchio, G. De Cataldo, C. De Marzo, O. Erriquez, C. Favuzzi, P. Fusco, N. Giglietto, P. Spinelli; **Bartol:** J. Petrakis; **Bologna:** S. Cecchini, G. Giacomelli, G. Mandrioli, A. Margiotta-Neri, P. Matteuzzi, L. Patrizii, F. Predieri, G.L. Sanzani, E. Scapparone, P. Serra Lugaresi, M. Spurio, V. Togo; **Boston:** S. Ahlen, R. Cormack, E. Kearns, S. Klein, G. Ludlam, A. Marin, C. Okada, J. Stone, L. Sulak, W. Worstell; **Caltech:** B. Barish, S. Coutu, J. Hong, E. Katsivounidis, S. Kyriazopoulou, G. Liu, R. Liu, D. Michael, C. Peck, N. Pignatano, K. Scholberg, J. Steele, C. Walter; **Drexel:** C. Lane, R. Steinberg; **Frascati:** G. Battistoni, H. Bilokon, C. Bloise, P. Campana, P. Cavallo, V. Chiarella, C. Forti, A. Grillo, E. Iarocci, A. Marini, V. Patera, F. Ronga, L. Satta, M. Spinetti, V. Valente; **Gran Sasso:** C. Gustavino, J. Reynoldson; **Indiana:** A. Habig, R. Heinz, L. Miller, S. Mufson, J. Musser, S. Nutter; **L'Aquila:** A. Di Credico, P. Monacelli; **Lecce:** P. Bernardini, G. Mancarella, D. Martello, O. Palamara, S. Petrera, P. Pistilli, A. Surdo; **Michigan:** E. Diehl, D. Levin, M. Longo, C. Smith, G. Tarlé; **Napoli:** M. Ambrosio, G. C. Barbarino, F. Guarino, G. Osteria; **Pisa:** A. Baldini, C. Bemporad, F. Cei, G. Giannini,* M. Grassi, R. Pazzi; **Roma:** G. Auriemma,** S. Bussino, C. Chiera, P. Chrysicopoulou, A. Corona, M. DeVincenzi, L. Foti, E. Lamanna, P. Lipari, G. Martellotti, G. Rosa, A. Sciubba, M. Severi; **Sandia Labs:** P. Green; **Texas A&M:** R. Webb; **Torino:** V. Bisi, P. Giubellino, A. Marzari Chiesa, M. Maserà, M. Monteno, S. Parlati, L. Ramello, M. Sitta

*Univ. di Trieste

**Univ. della Basilicata

A measurement of the underground muon decoherence function
has been performed using multiple muon events collected by the
MACRO experiment at Gran Sasso.

INTRODUCTION

Multiple muons detected underground by the MACRO experiment at Gran Sasso come mainly from the decay of mesons produced by primaries having an energy per nucleon greater than 100 TeV.

Here we present the results obtained from the analysis of data on the spatial separation of muon pairs in multiple muon events collected by MACRO in 1989 and 1990. We have developed a detector-independent analysis by correcting the measured μ -pair distribution for the detector efficiency dependence on μ -pair spacing and μ incidence angle. We use this analysis to compare the observed muon separation distribution with expectations from a Monte Carlo based on the parameterizations of recent results of experiments at hadron colliders.¹ A knowledge of the correct lateral distribution of muons is important in the study of the composition of cosmic ray primaries.²

DATA SELECTION AND PROCESSING

The MACRO detector is located in Hall B of the Gran Sasso underground laboratory.^{3,4} MACRO tracking is performed with streamer tubes, which are distributed on 10 horizontal planes, separated by CaCO_3 rock absorbers, and on six planes on each vertical wall. Two projective views are digitally read out, each with a spatial resolution of about 1.1 cm. Tracks on the different views can be associated in space in the majority of cases, depending on spatial separation and multiplicity. This permits the reconstruction of the distance between muons starting from their projective views.

The analysis presented here is based on events taken with one supermodule (SM) corresponding to about 4,900 hours live time, and two supermodules corresponding to about 2,300 hours. About 73,500 multiple muon events have been

collected in these periods. The analysis of muon pair separation has been restricted to events with zenith angles smaller than 60 degrees to be consistent with the muon sample generated by the Monte Carlo program.¹ Secondary particles produced by interactions in the surrounding rock or in the detector absorber are rejected by parallelism cuts. These cuts select those muon pairs having a relative angle less than 3 degrees and less than 3σ on the slope of the track with the largest error. The resulting total number of unambiguously reconstructed muon pairs is 20,150 for the one SM sample, and 31,400 for the two SM sample.

Fig. 1 shows the measured distributions of muon separation for the two different data samples in 40 cm bins. The bin size is far greater than our 5 mm resolution.

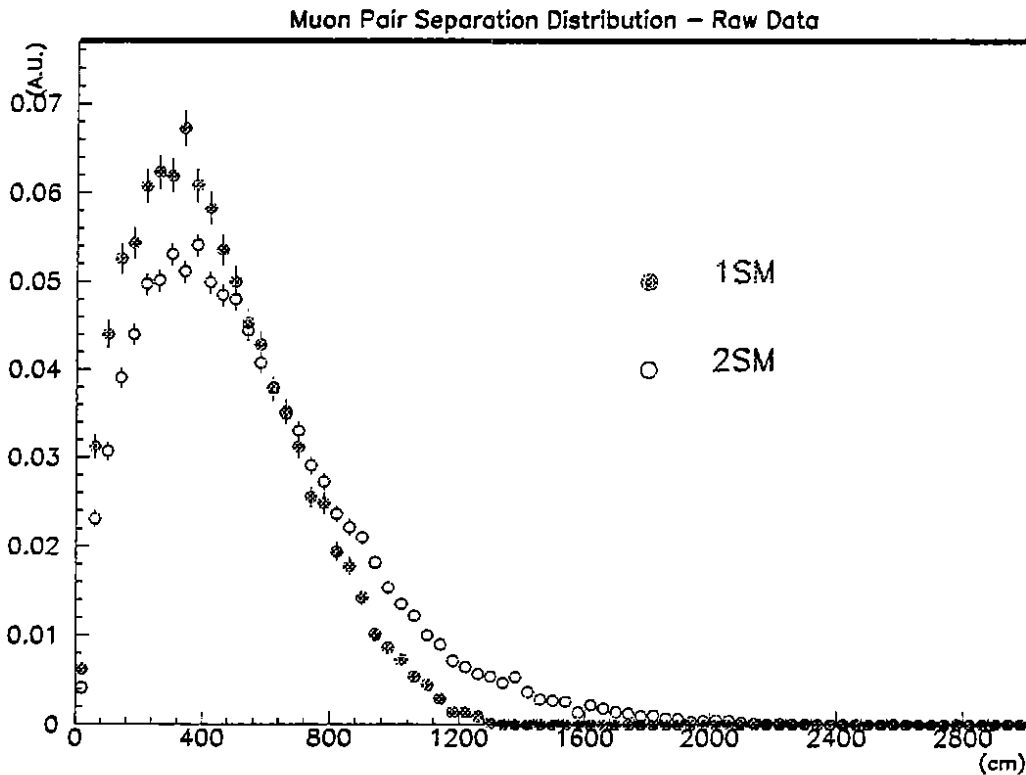


Figure 1 Separation distribution of muon pairs collected with one (solid circles) and two (open circles) SM. The ordinate is in arbitrary units (A.U.).

DETECTOR INDEPENDENT ANALYSIS

For comparing observations with calculations based upon hadronic interaction models, it is necessary to remove the effects of a finite detector size. There are three important effects that must be taken into account: the projected area of the detector depends upon an event's spatial direction; the detection probability of a muon pair in an event depends upon both its separation and position; and, the observed multiplicity of an event is usually smaller than its true multiplicity.

The calculation of the detector projected area is straightforward. But that of the detection probability as a function of separation and position is more subtle and two different techniques were used. One was a purely Monte Carlo calculation giving the percentage of fully reconstructed pairs for each angle and muon distance. The other used experimentally observed events and randomized their centroid locations. The results of these two methods are in agreement.

The last effect is easily corrected for by including each event with unit weight, i.e., each pair in an event with **observed** multiplicity N is entered with a weight $\frac{2}{N(N-1)}$. (This is a multiplicative weight applied after the weight due to the first two effects is determined.)

Our results can be compared with a Monte Carlo model calculation in which each event is similarly entered with unit weight. In performing Monte Carlo predictions, we obtain curves which are directly comparable to our data and which are sensitive to hadronic interactions of few hundred TeV. A comparison of our results with experiments at different depths is difficult because of the different muon energy thresholds.

Fig. 2 shows the superposition of the corrected decoherence curve for one SM and for two SM, normalized in the common separation interval (12 m): the consistency of the results validates our finite detector size correction procedures and allows us to combine the entire sample.

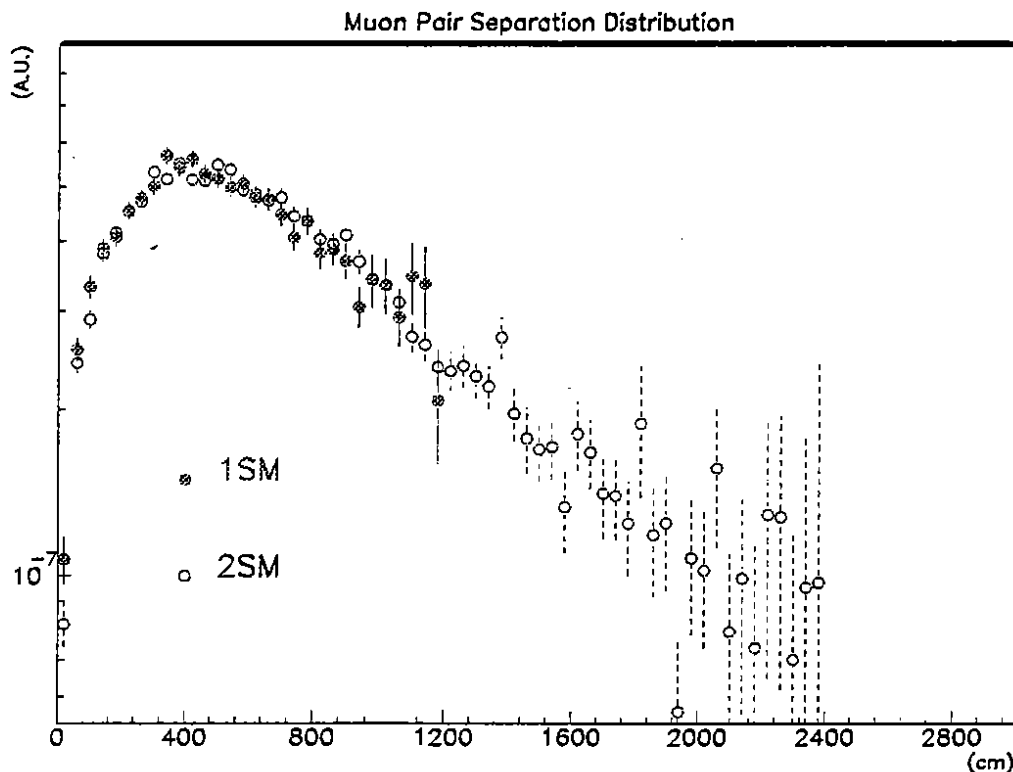


Figure 2. Decoherence curve obtained after correction for the finite size of the detector. Solid and open circles refer to the results obtained with 1 and 2 SM respectively.

COMPARISON WITH MONTE CARLO AND CONCLUSIONS

The parameterization published in Ref. 1 has been used to generate multiple muon events at the Gran Sasso site, and a Monte Carlo simulation of the decoherence function has been obtained. A few commonly considered primary spectra have been tested. As expected, they do not exhibit any detectable difference as far as muon separation is concerned, so that in the following we shall consider only the CMC model.⁵ The primary energy has been sampled in the range 2 TeV to 10^5 TeV, the shower axis is chosen isotropically, and for each direction the rock depth is calculated from the Gran Sasso map. The muon multiplicity and the distance of muons from the shower axis are generated according to the quoted parameterizations¹ based on data taken by recent collider experiments.⁶ Multiple scattering in the rock, which affects the muon separation underground, has also been taken into account. Each generated event, irrespective of its multiplicity, enters with unit weight in the decoherence function. Fig. 3 shows the superposition of experimental results and Monte Carlo. A reasonable agreement of the shapes of the two distribution is obtained, confirming the model of the hadronic interaction assumed in Ref. 1 within the sensitivity of the present analysis.

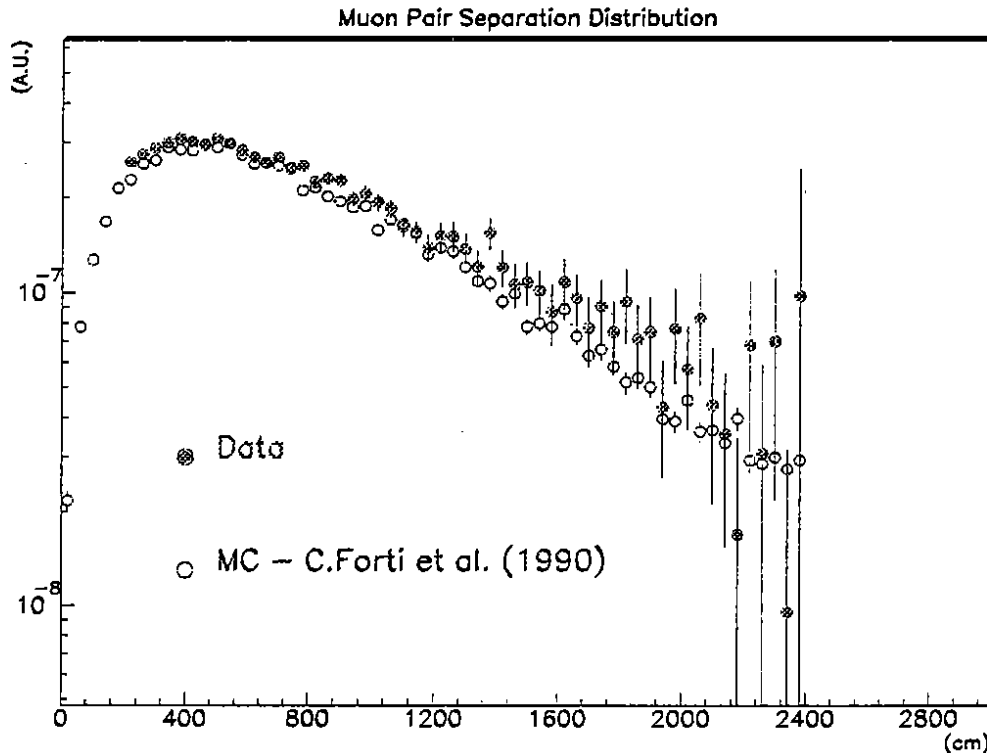


Figure 3. The measured decoherence function (solid circles), compared with the prediction of the Monte Carlo¹ (open circles).

MACRO is running now with six supermodules, and soon large data samples (a few $\times 10^5$ multiple μ events) will be analysed. Distances up to 75 m will be measured, and we will be able to study the interesting region of high p_t events.

REFERENCES

1. C. Forti et al., *Phys. Rev. D* **42**, 3668 (1990).
2. MACRO Collaboration, paper OG6.1-2, these proceedings.
3. MACRO Collaboration, proc. of the XXI ICRC, Adelaide (Australia), Vol. **10**, p. 256 (1990).
4. S.P. Ahlen et al., *Phys. Lett.* **249B**, 149 (1990), and references therein.
5. J. Kempa and J.Wdowczyk, *Nucl. Phys.* **9**, 1271 (1983).
6. G.J. Alner et al., *Phys. Lett.* **160B**, 199 (1985) and **167B**, 476 (1986).

Study of the Primary Cosmic Ray Composition with the MACRO Experiment at Gran Sasso

The MACRO Collaboration

Bari: R. Bellotti, F. Cafagna, M. Calicchio, G. De Cataldo, C. De Marzo, O. Enriquez, C. Favuzzi, P. Fusco, N. Giglietto, P. Spinelli; **Bartol:** J. Petrakis; **Bologna:** S. Cecchini, G. Giacomelli, G. Mandrioli, A. Margiotta-Neri, P. Matteuzzi, L. Patrizii, F. Predieri, G.L. Sanzani, E. Scapparone, P. Serra Lugaresi, M. Spurio, V. Togo; **Boston:** S. Ahlen, R. Cormack, E. Kearns, S. Klein, G. Ludlam, A. Marin, C. Okada, J. Stone, L. Sulak, W. Worstell; **Caltech:** B. Barish, S. Coutu, J. Hong, E. Katsuvounidis, S. Kyriazopoulou, G. Liu, R. Liu, D. Michael, C. Peck, N. Pignatano, K. Scholberg, J. Steele, C. Walter; **Drexel:** C. Lane, R. Steinberg; **Frascati:** G. Battistoni, H. Bilokon, C. Bloise, P. Campana, P. Cavallo, V. Chiarella, C. Forti, A. Grillo, E. Iarocci, A. Marini, V. Patera, F. Ronga, L. Satta, M. Spinetti, V. Valente; **Gran Sasso:** C. Gustavino, J. Reynoldson; **Indiana:** A. Habig, R. Heinz, L. Miller, S. Mufson, J. Musser, S. Nutter; **L'Aquila:** A. Di Credico, P. Monacelli; **Lecce:** P. Bernardini, G. Mancarella, D. Martello, O. Palamara, S. Petrera, P. Pistilli, A. Surdo; **Michigan:** E. Diehl, D. Levin, M. Longo, C. Smith, G. Tarlé; **Napoli:** M. Ambrosio, G. C. Barbarino, F. Guarino, G. Osteria; **Pisa:** A. Baldini, C. Bemporad, F. Cei, G. Giannini, * M. Grassi, R. Pazzi; **Roma:** G. Auriemma, ** S. Bussino, C. Chiera, P. Chrysicopoulou, A. Corona, M. DeVincenzi, L. Foti, E. Lamanna, P. Lipari, G. Martellotti, G. Rosa, A. Sciubba, M. Severi; **Sandia Labs:** P. Green; **Texas A&M:** R. Webb; **Torino:** V. Bisi, P. Giubellino, A. Marzari Chiesa, M. Maserà, M. Monteno, S. Parlati, L. Ramello, M. Sitta

*Univ. di Trieste

**Univ. della Basilicata

The analysis of multiple muon events collected with one MACRO supermodule (1013 h live time) and two supermodules (1195 h live time) is described. Muon multiplicity distributions are presented and compared with two primary cosmic ray composition models.

INTRODUCTION

The muon rates at different multiplicities measured in deep underground experiments are sensitive to the energy spectrum and chemical composition of primary cosmic ray nuclei at energies above 100 TeV. In this energy region direct measurements of composition are still poor because of extremely low fluxes. The sensitivity to composition arises from the fact that heavy cosmic ray nuclei are more effective than protons in producing multiple muons. The role of the primary hadronic interaction is of great importance when the size of the detector is not large enough to contain the muon bundle. In particular the transverse momentum distribution of the energetic secondaries largely determines the fraction of muons above threshold that hit the detector. This is discussed in a separate paper.¹

Given a model of high energy nucleus-nucleus interactions, it is possible to determine the composition on the basis of a comparison of muon multiplicity measurements with an accurate Monte Carlo simulation. If the muon lateral distribution is well known and the detector is large, the bias due to the finite size of the apparatus can be corrected.

The MACRO detector, located in the hall B of the Gran Sasso National Laboratory (with a minimum and average rock overburden of 3100 and 3800 MWE respectively) has dimensions of $72 \text{ m} \times 12 \text{ m} \times 4.8 \text{ m}$. It has a modular structure whose basic block is a "supermodule" of $12 \times 12 \times 4.8 \text{ m}^3$. A detailed description of the experimental apparatus is given elsewhere.²

In this paper we present an analysis of multiple muon events collected with one supermodule operating from March 4, 1990 through May 10, 1990 and with two supermodules operating from May 10, 1990 through July 19, 1990.

DATA SELECTION AND EVENT ANALYSIS

Muons are reconstructed separately on wire and strip views; alignment of at least 4 hits in different planes is required to define a track. Two independent projected multiplicities, N_W and N_S , in the wire and strip views, are obtained for each event. In most cases it is possible to associate tracks in the two views to reconstruct the muon tracks in three-dimensional space. 94% of muon pairs in all events having any multiplicity are unambiguously associated. The rate of reconstructed single muons with $N_W = N_S = 1$ is $116 \mu/\text{h}$ for the sample with one supermodule and $235 \mu/\text{h}$ with two supermodules.

In the present analysis, the runs have been selected according to the rate of reconstructed single muon events. At least $100 \mu/\text{h}$ for one supermodule and $200 \mu/\text{h}$ for two supermodules have been required in order to select run periods with good streamer tube system operation. Only runs with total live time $\geq 1 \text{ h}$ and dead time fraction $< 5 \%$ have been used to eliminate those runs with possible technical problems. Following these criteria the selected event samples correspond to 1013 h and 1195 h of total live time for one supermodule and two supermodules respectively. We also required the zenith angle of the muon bundles to be less than 60° . The fraction of events surviving this cut is $\sim 94 \%$.

The events have been subdivided into different subsamples according to the reconstructed multiplicities N_W and N_S . The true multiplicity of each event can be different from these two numbers for various reasons, such as a geometrical superposition of two or more tracks in a view.

A fraction of events was visually scanned in order to solve possible ambiguities. The basic scanning criterion to define a muon track was to demand at least 4 aligned hits in the horizontal planes. A range of different multiplicities has been assigned to complicated events (mainly events with showers) when the true multiplicity could not be unambiguously determined. This was done giving a constant fractional weight to each possible multiplicity within the range defined by the scanner.

All events with $N_W > 5$ or $N_S > 5$ have been scanned. All remaining events were scanned on a sampling basis. In this analysis a total of about 5000 events were scanned.

Table I. Muon multiplicities after scanning corrections. Corresponding live times are given in the text.

N_μ	1 SM	2 SM	N_μ	1 SM	2 SM
1	123900 ± 1300	268700 ± 6200	13	0.6 ± 0.6	5.8 ± 2.4
2	3920 ± 130	10400 ± 250	14	0.6 ± 0.6	4.3 ± 2.1
3	658 ± 45	1620 ± 69	15	1.3 ± 1.1	1.3 ± 1.1
4	148 ± 14	566 ± 35	16	0	1.7 ± 1.3
5	78 ± 10	201 ± 16	17	0	2.2 ± 1.5
6	38 ± 9	102 ± 10	18	1 ± 1	1.3 ± 1.1
7	15 ± 4	69 ± 9	19		0.5 ± 0.5
8	15 ± 4	39 ± 6	20		0.3 ± 0.3
9	7 ± 3	19 ± 4	21		0.3 ± 0.3
10	5 ± 2.2	11 ± 3	22		0.3 ± 0.3
11	3.5 ± 1.9	8.5 ± 2.9	...		0
12	1.3 ± 1.1	4.8 ± 2.2	27		1 ± 1

The results obtained in different periods of operation of the detector are reported in Table I. Only statistical errors, inclusive of scanning uncertainties, are reported in this table. The systematic error, estimated from a partial rescanning, is comparable to the statistical error. Fig. 1 shows the multimMuon rates for one supermodule and two supermodule event samples.

COMPARISON WITH MONTE CARLO PREDICTIONS

The interpretation of deep underground data requires a simulation including the primary hadronic interaction model, the air shower development and the propagation of muons through the rock. Simulations for an infinite size detector have already been developed.^{3,4,5} The results of these calculations are expressed in terms of parametrized formulas describing the main features of the muon bundles, i.e., their lateral distance and multiplicity distributions. These parameterizations can be used in Monte Carlo simulation programs in order to obtain predictions of multimMuon data on the actual detector. Some predictions based on numerical integration with a simplified description of the MACRO detector (box model) have been reported in Ref. 5.

We have undertaken a full Monte Carlo simulation with the following features:

- i) a physics generator including both the parameterizations of hadronic interactions and the characteristics (energy spectrum and elemental composition) of the primary cosmic radiation;
- ii) an accurate description of the rock depth distribution around the MACRO detector; and
- iii) a GEANT⁶ based simulation program describing the experimental apparatus in all its details (geometry and detector response) and producing data of the same format as for real events. These data have been processed using the standard offline chain of analysis, which permits an evaluation of both the MACRO acceptance and the reconstruction program efficiency.

Our results are insensitive to changes in the parameterization of the hadronic interaction model at fixed composition. We have adopted the parameterization of Ref. 5.

We have compared our experimental rates of multimunuons with two compositions given in literature: the Maryland⁷ (heavy) and LEC proton enhanced⁸ (light) compositions, as adjusted to give the same "all particle" spectrum in Ref. 9. The results of these simulations are shown in Fig. 2, compared with the experimental data with two supermodules. Error bars represent statistical errors on the data points and preliminary estimates of systematic uncertainties on the Monte Carlo points. A change of the rock overburden by 1% everywhere produces a shift of 70% in the rate for a multiplicity of 20 or more. The Monte Carlo predictions are normalized to the same number of events as experimentally observed, in order to reduce possible systematic biases not currently taken into account. Rates are plotted up to a maximum multiplicity value for which the statistical uncertainty on generated events does not exceed 25%.

Although the present analysis on muon multiplicities seems to show a preference towards lighter compositions, significant systematic uncertainties may still exist in the Monte Carlo calculations and the mapping of the overburden. Work is in progress to better understand systematic uncertainties.

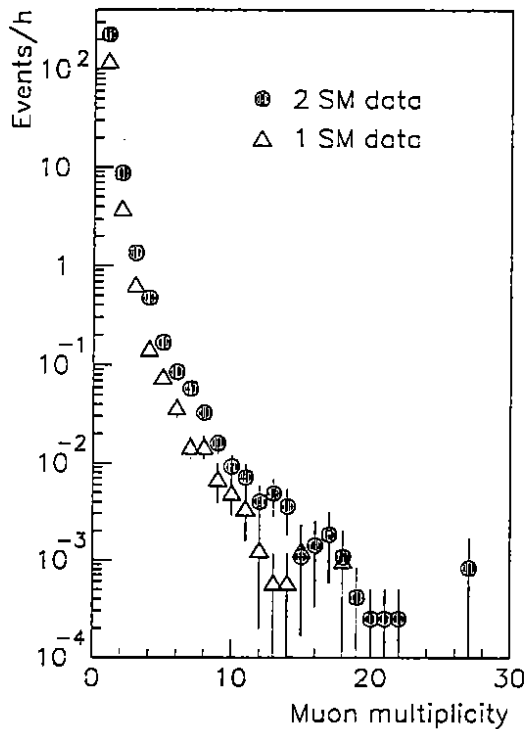


Figure 1. Distribution of multi-muon rates as a function of multiplicity for the one supermodule and two supermodule samples. Only statistical errors, inclusive of scanning uncertainties, are shown.

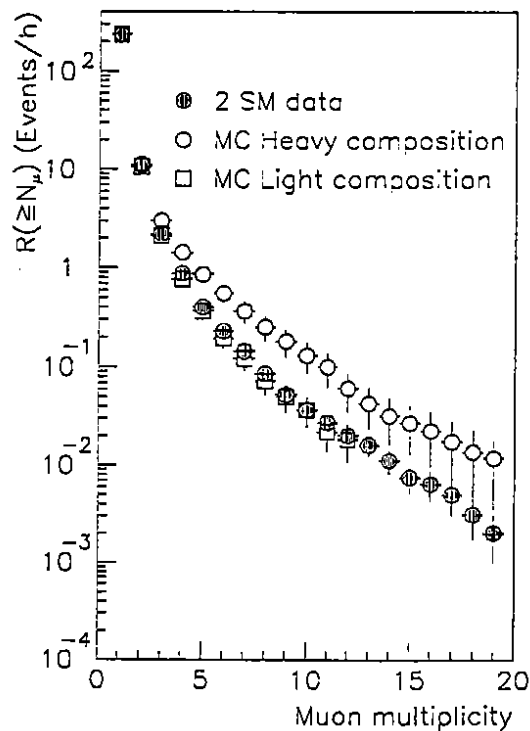


Figure 2. Comparison between the integral multiplicity distributions of two supermodule data and Monte Carlo predictions. The "Heavy" and "Light" composition models (described in the text) are not corrected for systematic errors.

REFERENCES

1. MACRO Collaboration, HE4.2-6, these proceedings.
2. M. Calicchio et al., *Nucl. Instr. and Meth.* **A264**, 18 (1988).
3. T.K. Gaisser and T. Stanev, *Nucl. Instr. and Meth.* **A235**, 183 (1985).
4. G. Bologna et al., *Nuovo Cimento* **8C**, 76 (1985).
5. C. Forti et al., *Phys. Rev.* **D42**, 3668 (1990).
6. R. Brun et al., "GEANT3 manual", CERN DD/EE/84-1.
7. J.A. Goodman et al., *Phys. Rev. Lett* **42**, 854 (1979).
8. C. Fichtel and J. Linsley, *Astrophys. Jour.* **300**, 474 (1986).
9. G. Auriemma et al., HE4.5-5, **9**, 362 (1990), in Proc. of XXI ICRC Conference, Adelaide, Australia.

A Search for Prompt Muons using the MACRO Detector at Gran Sasso

The MACRO Collaboration

Bari: R. Bellotti, F. Cafagna, M. Calicchio, G. De Cataldo, C. De Marzo, O. Erriquez, C. Favuzzi, P. Fusco, N. Giglietto, P. Spinelli; **Bartol:** J. Petrakis; **Bologna:** S. Cecchini, G. Giacomelli, G. Mandrioli, A. Margiotta-Neri, P. Matteuzzi, L. Patrizzii, F. Predieri, G.L. Sanzani, E. Scaparoni, P. Serra Lugaresi, M. Spurio, V. Togo; **Boston:** S. Ahlen, R. Cormack, E. Kearns, S. Klein, G. Ludlam, A. Marin, C. Okada, J. Stone, L. Sulak, W. Worstell; **Caltech:** B. Barish, S. Coutu, J. Hong, E. Katsuvounidis, S. Kyriazopoulou, G. Liu, R. Liu, D. Michael, C. Peck, N. Pignatano, K. Scholberg, J. Steele, C. Walter; **Drexel:** C. Lane, R. Steinberg; **Frascati:** G. Battistoni, H. Bilokon, C. Bloise, P. Campana, P. Cavallo, V. Chiarella, C. Forti, A. Grillo, E. Iarocci, A. Marini, V. Patera, F. Ronga, L. Satta, M. Spinetti, V. Valente; **Gran Sasso:** C. Gustavino, J. Reynoldson; **Indiana:** A. Habig, R. Heinz, L. Miller, S. Mufson, J. Musser, S. Nutter; **L'Aquila:** A. Di Credico, P. Monacelli; **Lecce:** P. Bernardini, G. Mancarella, D. Martello, O. Palamara, S. Petrera, P. Pistilli, A. Surdo; **Michigan:** E. Diehl, D. Levin, M. Longo, C. Smith, G. Tarié; **Napoli:** M. Ambrosio, G. C. Barbarino, F. Guarino, G. Osteria; **Pisa:** A. Baldini, C. Bemporad, F. Cei, G. Giannini, M. Grassi, R. Pazzi; **Roma:** G. Auriemma, S. Bussino, C. Chiera, P. Chrysicopoulou, A. Corona, M. DeVincenzi, L. Foti, E. Lamanna, P. Lipari, G. Martellotti, G. Rosa, A. Sciubba, M. Severi; **Sandia Labs:** P. Green; **Texas A&M:** R. Webb; **Torino:** V. Bisi, P. Giubellino, A. Marzari Chiesa, M. Maserà, M. Monteno, S. Parlati, L. Ramello, M. Sitta

*Univ. di Trieste

**Univ. della Basilicata

In this paper we present the energy spectrum and the distribution of a sample of muon tracks observed in MACRO. We have investigated these distributions to search for a prompt component, such as would arise from charmed hadro-production.

MACRO¹ is a large area underground detector capable of precise muon tracking which has been operating in Hall B of the Gran Sasso Laboratory since February 27, 1989.

The full detector is still under construction and it will eventually consist of six lower and six upper supermodules. Each lower supermodule has dimensions $12 \times 12 \times 4.8 \text{ m}^3$ and provides an acceptance for downward isotropic particle fluxes of $\approx 800 \text{ m}^2 \text{ sr}$. It consists of a sandwich array of two layers of liquid scintillation counters (top and bottom) and ten layers of streamer tubes each separated by 32 cm of rock absorber. The sides and the two extreme ends of the detector are covered with one layer of scintillator and six layers of streamer tubes. The streamer tube system consists of approximately 5000 wires per supermodule.

For this analysis we have selected two periods of data taking, the first from February 27 to May 30, 1989 and the second from March 4 to May 10, 1990.

We have selected runs with total live time $\geq 3 \text{ h}$, with $< 5\%$ dead time and with $\geq 100 \mu\text{h}$ reconstructed. The standard run duration was 8 hours and the dead time was approximately 1-2%. After these selections, we had a total live time of 3,279 h during which 328,000 muon tracks were reconstructed.

For zenith angles $\theta \leq 53^\circ$, we know the elevation map of the Gran Sasso mountain, its average density ($\bar{\rho} = 2.71 \pm 0.05 \text{ g cm}^{-3}$), and its chemical composition² (26% Ca + 51.5% O + 12.5% C + 9% Mg + 1% Si). We have included in this analysis

only muons inside this vertical cone in order to be able to estimate accurately the slant depth h crossed by each detected muon.

The observed distribution of the muon sample was converted into uncorrelated muon intensities in $\text{m}^{-2} \text{s}^{-1} \text{sr}^{-1}$, plotted in Fig. 1, with the formula:

$$I_{\text{exp}}(h, \cos \theta) = \left(\frac{1}{\Delta t \Delta \Omega \epsilon} \right) \frac{\sum_j N_j m_j}{\sum_j A_j} \quad (1)$$

where Δt is the live time, N_j is the observed number of events for each of the bins at slant depth h , m_j is the number of muons per event, A_j is the projected area of the detector, and ϵ is the trigger and reconstruction efficiency. In this equation the sums have been taken over all bins for which the slant depth is within h and $h + \Delta h$ and the zenith angle is within $\cos \theta$ and $\cos \theta + \Delta \cos \theta$. For this data sample the efficiency ϵ was estimated from the data to be 98% and is independent of direction.

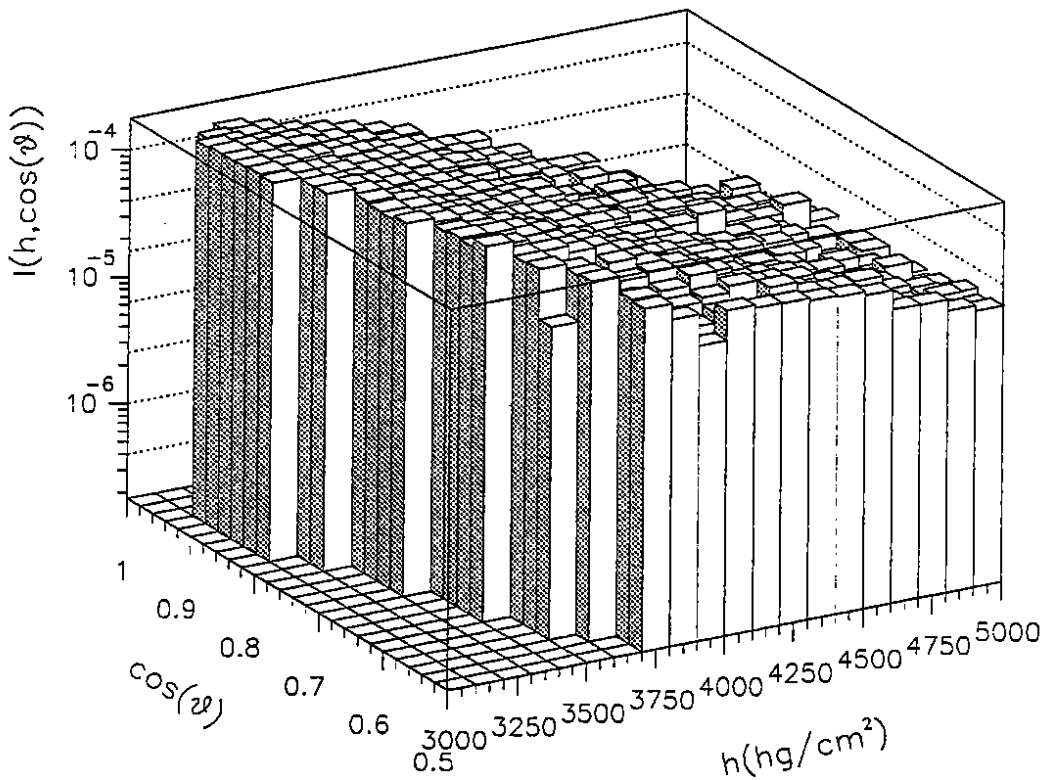


Figure 1. Intensity of muons binned with $\Delta \cos \theta = 0.02$ and $\Delta h = 100 \text{ hg cm}^{-2}$.

In Fig. 2 we show the $\sec \theta$ distribution of our experimental data for each bin in slant depth between 3100 and 4900 hg cm^{-2} . In the same Fig. 2 we compare the observed muon intensities with the ones calculated from a best fit theoretical spectrum of the form:

$$\Phi = A_{\pi,k} G_{\pi,k} E_{\mu}^{-\gamma_{\pi,k}} + A_{pr} E_{\mu}^{-\gamma_{pr}} \quad (2)$$

where Φ is in $\text{m}^{-2} \text{s}^{-1} \text{sr}^{-1} \text{TeV}^{-1}$ and E_{μ} is in TeV. $G_{\pi,k}$ takes into account the $\cos \theta$ dependence of the pion and kaon decay in the atmosphere. According to a standard reference⁴ this dependence is well approximated by the formula:

$$G_{\pi,k} = \frac{1}{1 + \frac{1.1 E_{\mu} \cos \theta}{0.115 \text{ TeV}}} + \frac{0.054}{1 + \frac{1.1 E_{\mu} \cos \theta}{0.850 \text{ TeV}}} \quad (3)$$

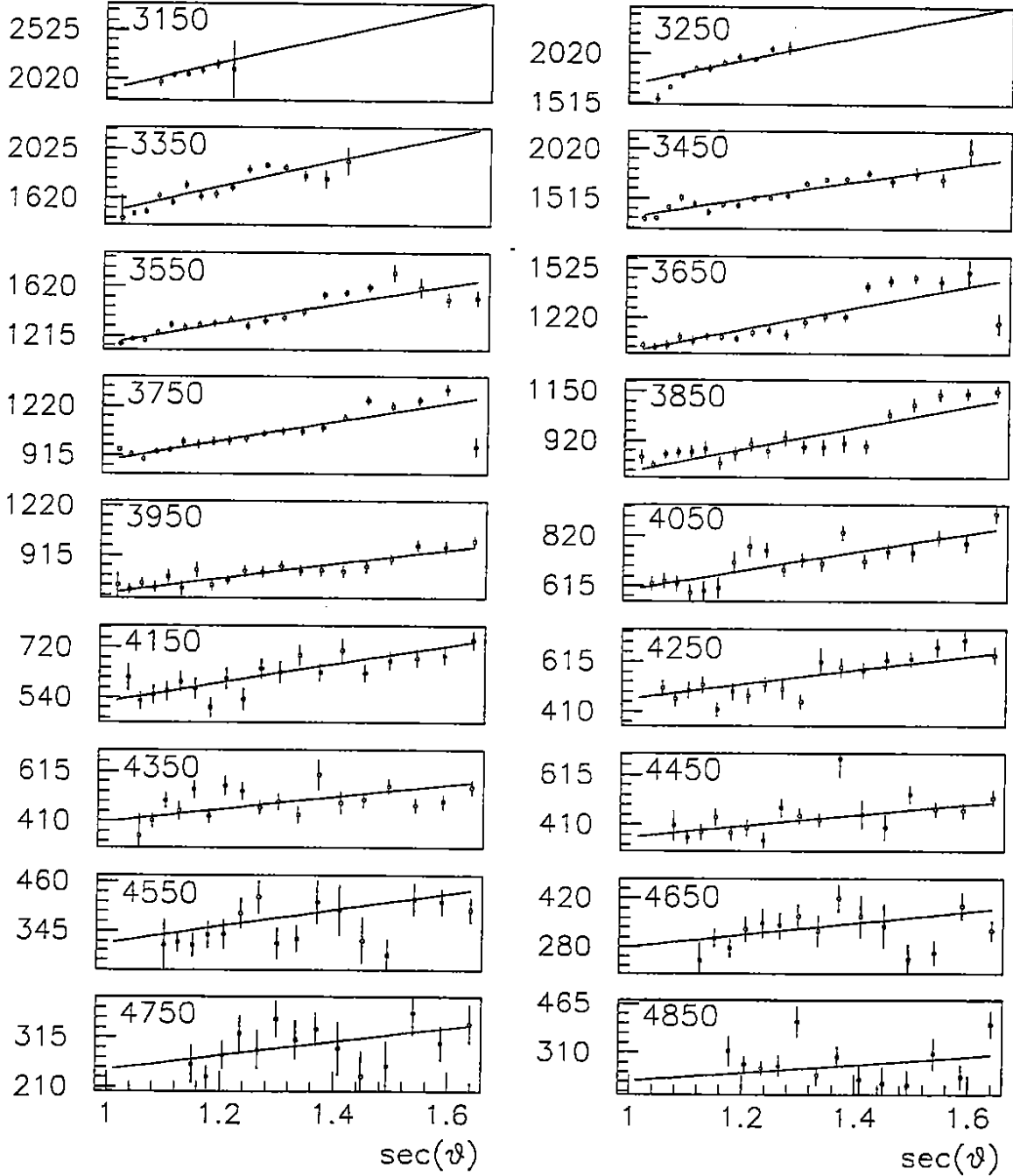


Figure 2. Intensity of muons versus $\sec \theta$ for slant depth between 3100 and 4900 hg cm^{-2} . Errors shown are statistical. Systematic uncertainties are not included.

Using MINUIT we have minimized the $\chi^2 = (I_{\text{exp}} - I_{\text{th}})^2 / \sigma_{\text{stat}}^2$ with

$$I_{\text{th}}(h, \cos \theta) = \int P_{\text{surv}}(h, E_\mu) \Phi(E_\mu, \cos \theta) dE_\mu \quad (4)$$

as a function of the four parameters $A_{\pi,k}$, $\gamma_{\pi,k}$, A_{pr} and γ_{pr} . In this formula $P_{\text{surv}}(h, E_\mu)$ is the probability that a muon of initial energy E_μ reaches the detector. We have calculated this probability with GEANT 3.13 over a grid of 25 values of E_μ harmonically spaced in the interval from 1 TeV to 10 TeV, in order to minimize the interpolation error in the evaluation of the integral in Eq. 4.

The best fit was obtained with $A_{\pi,k} = (1.0 \pm 0.1) \times 10^{-2}$, $\gamma_{\pi,k} = 2.78 \pm 0.11$, $A_{\text{pr}} = (0.9 \pm 0.5) \times 10^{-4}$, and $\gamma_{\text{pr}} = 2.4 \pm 0.4$, but the corresponding value of χ^2 is 2.3 per degree of freedom (DoF).

If we do not include a prompt component, the best fit is obtained for $A_{\pi,k} = (1.0 \pm 0.2) \times 10^{-2}$ and $\gamma_{\pi,k} = 2.54 \pm 0.02$ with a χ^2 of 2.6 per DoF. Therefore we conclude from this preliminary analysis that our data do not show definitive evidence for a prompt component.

If we minimize $\chi'^2 = (I_{\text{exp}} - I_{\text{th}})^2 / (\sigma_{\text{stat}}^2 + \sigma_{\text{syst}}^2)$ where σ_{syst}^2 is the error arising from the uncertainty in the slant depth (which we estimate to be $\delta h/h = 1\%$) we obtain a $\chi'^2 = 0.89/\text{DoF}$ for the above given parameters with the prompt component and a $\chi'^2 = 1/\text{DoF}$ if we do not include the prompt component. The small difference in the χ^2 values does not support the presence of a prompt component, which is likely masked by the 1% systematic error of our determination of the slant depth, which we plan to reduce in the future. Future study must also be done on other possible systematic effects in the data.

In conclusion we estimate, from this preliminary analysis, that the integral flux of prompt muons above 1.5 TeV is lower than $10^{-8} \text{ cm}^{-2} \text{ s}^{-1} \text{ sr}^{-1}$ with 90% confidence level. This upper limit is obtained by propagation of the error in the fitted parameters, given in Eq. 2, taking into account the correlations existing between them.

REFERENCES

1. G. Battistoni et al.; *Nucl. Instr. and Meth.* **A270**, 185 (1988).
2. S.P. Ahlen et al.; *Phys. Lett.* **B249**, 149 (1990).
3. Y. Muraki et al., *Phys. Rev.* **D28**, 40 (1983).
4. T.K. Gaisser; "Cosmic Rays and Particle Physics," Cambridge University Press, Cambridge, p. 71 (1990).

Stellar Gravitational Collapse Detection by MACRO: Characteristics and Results

The MACRO Collaboration

Bari: R. Bellotti, F. Cafagna, M. Calicchio, G. De Cataldo, C. De Marzo, O. Erriquez, C. Favuzzi, P. Fusco, N. Giglietto, P. Spinelli; **Bartol:** J. Petrakis; **Bologna:** S. Cecchini, G. Giacomelli, G. Mandrioli, A. Margiotta-Neri, P. Matteuzzi, L. Patrizii, F. Predieri, G.L. Sanzani, E. Scapparone, P. Serra Lugaresi, M. Spurio, V. Togo; **Boston:** S. Ahlen, R. Cormack, E. Kearns, S. Klein, G. Ludlam, A. Marin, C. Okada, J. Stone, L. Sulak, W. Worstell; **Caltech:** B. Barish, S. Coutu, J. Hong, E. Katsivounidis, S. Kyriazopoulou, G. Liu, R. Liu, D. Michael, C. Peck, N. Pignatano, K. Scholberg, J. Steele, C. Walter; **Drexel:** C. Lane, R. Steinberg; **Frascati:** G. Battistoni, H. Bilokon, C. Bloise, P. Campana, P. Cavallo, V. Chiarella, C. Forti, A. Grillo, E. Iarocci, A. Marini, V. Patera, F. Ronga, L. Satta, M. Spinetti, V. Valente; **Gran Sasso:** C. Gustavino, J. Reynoldson; **Indiana:** A. Habig, R. Heinz, L. Miller, S. Mufson, J. Musser, S. Nutter; **L'Aquila:** A. Di Credico, P. Monacelli; **Lecce:** P. Bernardini, G. Mancarella, D. Martello, O. Palamara, S. Petrera, P. Pistilli, A. Surdo; **Michigan:** E. Diehl, D. Levin, M. Longo, C. Smith, G. Tarlé; **Napoli:** M. Ambrosio, G. C. Barbarino, F. Guarino, G. Osteria; **Pisa:** A. Baldini, C. Bemporad, F. Cei, G. Giannini, M. Grassi, R. Pazzi; **Roma:** G. Auriemma, S. Bussino, C. Chiera, P. Chrysicopoulou, A. Corona, M. DeVincenzi, L. Foti, E. Lamanna, P. Lipari, G. Martellotti, G. Rosa, A. Sciubba, M. Severi; **Sandia Labs:** P. Green; **Texas A&M:** R. Webb; **Torino:** V. Bisi, P. Giubellino, A. Marzari Chiesa, M. Maserà, M. Monteno, S. Parlati, L. Ramello, M. Sitta

*Univ. di Trieste

**Univ. della Basilicata

The first of twelve MACRO supermodules has been sensitive to a stellar gravitational collapse since spring '89. In this paper we discuss results from the 44 tonnes of liquid scintillator which have been instrumented to search for stellar gravitational collapse.

INTRODUCTION

The first of the MACRO detector ^{1,2} supermodules (SM1) has been operational since spring 1989. The detection of $\bar{\nu}_e$ -bursts from collapsing stars ($\langle E_{\bar{\nu}_e} \rangle \approx 10$ MeV, the $\bar{\nu}_e$ -burst duration ≈ 10 s) is based on $\bar{\nu}_e$ -interactions in the liquid scintillation counter system, via the primary reaction $\bar{\nu}_e + p \rightarrow n + e^+$, followed by delayed neutron capture in hydrogen $n + p \rightarrow \gamma + d$ with $E_\gamma = 2.2$ MeV. A search for stellar gravitational collapse was presented at the 1990 Adelaide I.C.R.C.² This paper reports on detector improvements and on subsequent data taking and analysis.

THE SCINTILLATION COUNTER SYSTEM

Each of the six lower MACRO supermodules (12 m \times 12 m \times 4.8 m) has two horizontal layers composed of 16 scintillation counters each; vertical counters cover the sides of the supermodule (21 counters for the 3 sides of SM1). The horizontal counters were used for the stellar collapse search (total scintillator mass ≈ 44 tons); vertical counters were only used for improving the cosmic ray rejection. Each horizontal liquid scintillator tank is 12 m long and has two 20 cm diameter phototubes at each end; the light transmission along the counter is approximately exponential with $\lambda_{att} \approx 12$ m. The determination of a low energy event position

and energy is based on the measurement of light arrival times and light intensities at the two counter ends.

THE STELLAR COLLAPSE ELECTRONICS

Two main background sources are present: cosmic rays and the natural radioactivity at the experimental site. Cosmic rays can be largely rejected since they are recognized as "tracks" crossing MACRO. The natural radioactivity background spectrum (mostly photons) is concentrated at low energies ($E < 5$ MeV). MACRO stellar collapse electronics performs the following functions:

- 1) It provides a trigger for events with an associated energy $E > E_{\text{pth}}$, the primary energy threshold, in ≈ 80 ns. Typical E_{pth} values are $5 < E_{\text{pth}} < 7$ MeV.
- 2) It lowers the energy threshold for that counter (and for the adjacent counters) to a secondary energy threshold $E_{\text{sth}} \approx 1.5$ MeV for a time ≈ 1 ms after a primary event in a counter. Secondary events occurring during this time are recorded (a maximum of 14 events), thus allowing the detection of possible 2.2 MeV γ 's from delayed neutron capture in hydrogen.
- 3) It measures with high accuracy ($\sigma \approx 1$ ns) both the time of each event relative to the experimental atomic clock standard time and the time difference between the signals from the two counter ends.
- 4) It digitizes and stores waveforms (100 MHz) relative to the primary and secondary events. These waveforms and the time information are used for the off-line event energy and position reconstruction.

THE ENERGY SCALE DETERMINATION AND CALIBRATION METHODS

An absolute calibration of the energy scale is obtained by analyzing cosmic ray μ 's, which have an energy loss ≈ 40 MeV in a MACRO counter. For relative calibration and test purposes, MACRO uses a variable intensity UV-light laser and an optical fiber system. Unavoidable non-linearities over a large energy range and the small cosmic ray rate ($R \approx 1 \text{ m}^{-2} \text{ h}^{-1}$) suggest the need for an independent absolute energy calibration at low energies ($1 < E < 10$ MeV). This was obtained by the use of a low intensity Am/Be source, a n and γ -ray emitter via the reaction ${}^9\text{Be}(\alpha, \gamma \text{n}) {}^{12}\text{C}$ with $E_\gamma = 4.44$ MeV, externally applied to the scintillation counters³. The 2.2 MeV late signal from n-capture, which occurs in $\approx 180 \mu\text{s}$, is a unique signature to identify $\bar{\nu}_e$ -events.

Fig. 1 shows the energy spectrum when the Am/Be source is applied to a MACRO counter; the 4.44 MeV and the 2.2 MeV γ -lines are both visible. The

experimental data are compared with the ones obtained (solid histogram in Fig. 1a) by a Monte Carlo calculation. This calculation simulates the Am/Be source emission, γ absorption and detection, n-moderation (by n-p and n-C scattering), n-capture in the liquid scintillator, and the counter geometry. A simultaneous fit to the γ -lines of Fig. 1 gives a measurement of the energy resolution: $\sigma_E \approx 0.6$ MeV at $E = 4.44$ MeV. The resolution in longitudinal position along the counter for the 2.2 MeV γ -ray, obtained by the (uncollimated) Am/Be source, is $\sigma_z < 1$ m. The efficiency for delayed n-capture detection following a primary $\bar{\nu}_e$ -event in a MACRO counter is $\approx 25\%$.

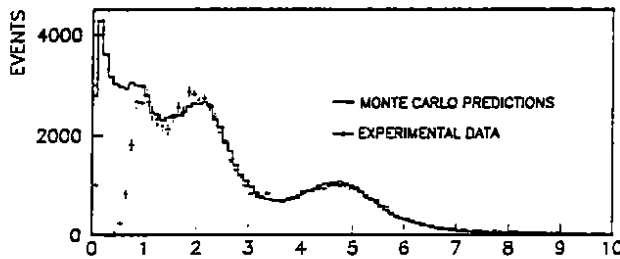


Fig. 1a. Energy spectrum for Am/Be source events. The 4.44 and the 2.2 MeV γ -lines are visible. The full-line histogram is the one of the Monte Carlo simulation.

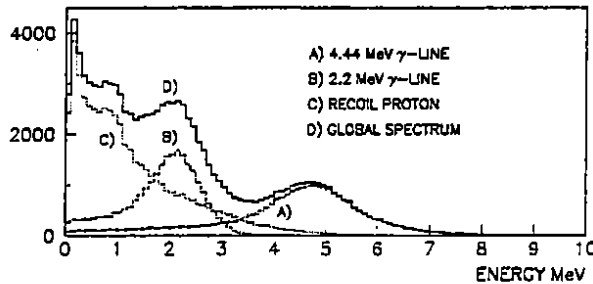


Fig. 1b. The decomposition of the Monte Carlo global result into predictions for different contributing processes.

5. THE "ON-LINE MONITOR"

Since stellar gravitational collapse data are collected in association with a rather low energy threshold, they are useful for monitoring the correct behavior of the scintillation counters and the associated electronics. An example of such a monitor is presented in Fig. 2: rates, event multiplicities, etc. are continuously recorded. In case of "anomalies" of whatever nature (stellar collapse or apparatus misbehavior) an alarm is generated; this allows a prompt, more refined analysis.

After gaining sufficient experience on the performance of such a monitor, one could transform this device as a real "Supernova Watcher" which might be used to alert, within a few hours, observers interested in studying the early stages of a new supernova.

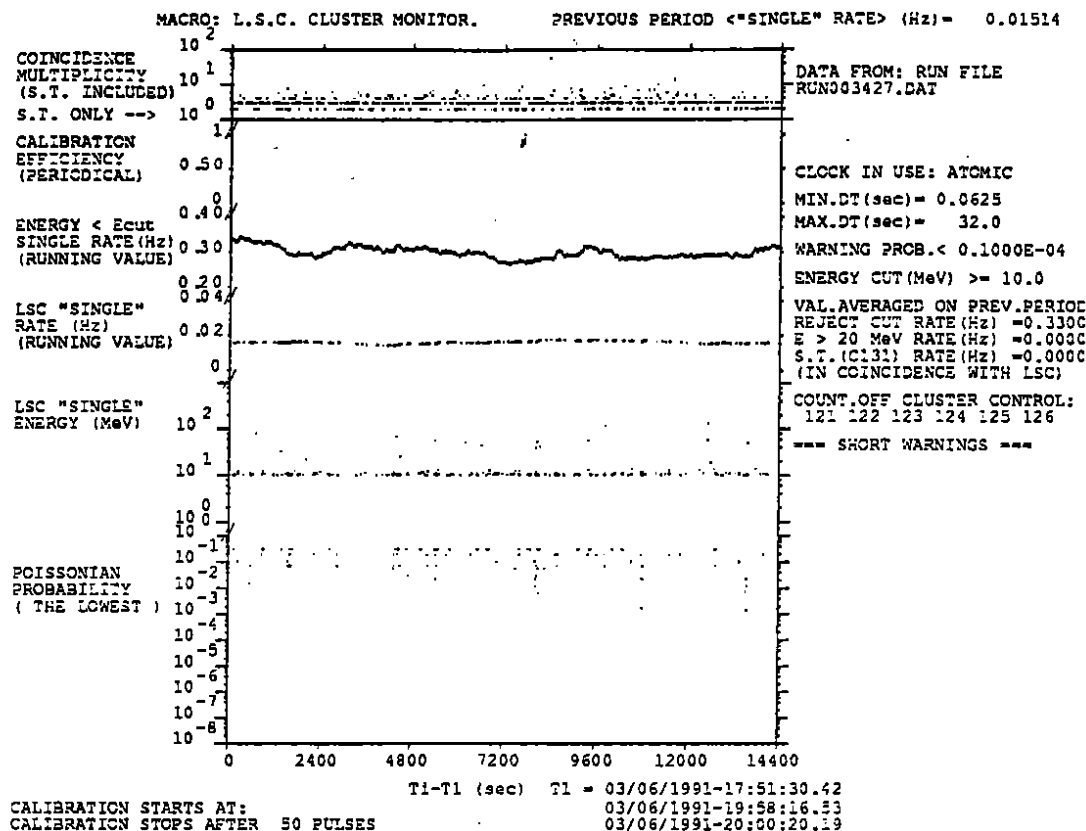


Fig. 2 The on-line monitor. Rates, event multiplicities, etc. are continuously recorded.

DATA ANALYSIS

We present the data collected during a period of about 14 months, from March 31, 1990 to June 4, 1991. The live time of SM1 during this period was $\approx 84\%$ due to interventions for regular maintenance; this problem will be avoided in the future when most of MACRO will be active even in case of repairs on one of the SM's. Events with $E > 10$ MeV were used in this analysis. After applying simple cosmic ray μ rejection criteria which make use of the information from all counters and of the μ -trigger signal from the MACRO streamer tube system¹, the final rate obtained was ≈ 15 mHz. We have searched for event clusters within sliding 2 s bins. The resulting multiplicity distribution is shown in Fig. 3 along with the expected Poisson distribution corresponding to the measured rate (histogram). No cluster with more than 3 events was found. If a stellar gravitational collapse equivalent to the one from SN1987A had occurred at the galactic center, it would have produced ≈ 8 detected events in a 2 s time window. Fig. 4 shows the number of times in which clusters of multiplicity 1, 2, 3, or 4 occurred vs. the cluster duration. The expectations according to Poisson statistics are also shown.

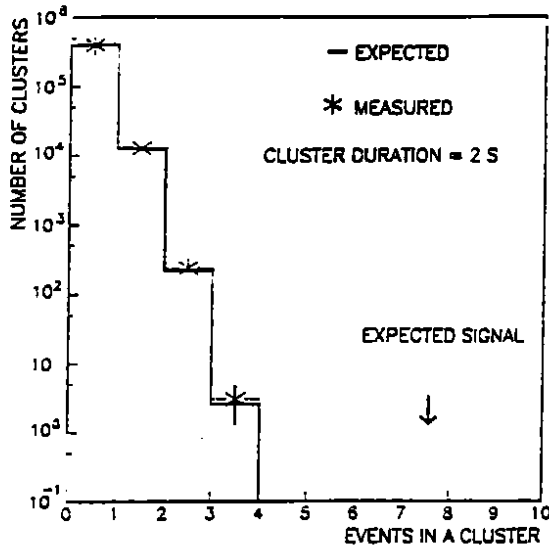


Fig. 3. Number of clusters vs. the number of events in a cluster; the cluster duration is 2 s. Data (*) and expectations (histogram) for the 14 month period.

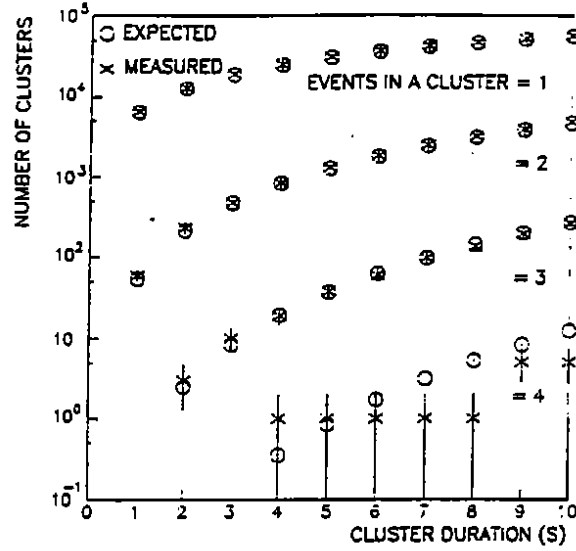


Fig. 4. Number of clusters vs. cluster duration for different number of events in a cluster. Data (*) and expectations (o) for the 14 months period.

REFERENCES

1. The MACRO Collaboration, *Nucl. Instr. & Meth. A* **264**, 18 (1988).
2. The MACRO Collaboration, Proc. of the XXI I.C.R.C., Adelaide (1990).
3. A. Baldini et al., *Nucl. Instr. & Meth.* (1991), in print.

Search for Nuclearites with the MACRO Detector

MACRO Collaboration

Bari: R. Bellotti, F. Cafagna, M. Calicchio, G. De Cataldo, C. De Marzo, O. Erriquez, C. Favuzzi, P. Fusco, N. Giglietto, P. Spinelli; **Bartol:** J. Petrakis; **Bologna:** S. Cecchini, G. Giacomelli, G. Mandrioli, A. Margiotto-Neri, P. Matteuzzi, L. Patrizii, F. Predieri, G.L. Sanzani, E. Scaparoni, P. Serra Lugaresi, M. Spurio, V. Togo; **Boston:** S. Ahlen, R. Cormack, E. Kearns, S. Klein, G. Ludlam, A. Marin, C. Okada, J. Stone, L. Sulak, W. Worstell; **Caltech:** B. Barish, S. Coutu, J. Hong, E. Katsuvounidis, S. Kyriazopoulou, G. Liu, R. Liu, D. Michael, C. Peck, N. Pignatano, K. Scholberg, J. Steele, C. Walter; **Drexel:** C. Lane, R. Steinberg; **Frascati:** G. Battistoni, H. Bilokon, C. Bloise, P. Campana, P. Cavallo, V. Chiarella, C. Forti, A. Grillo, E. Iarocci, A. Marini, V. Patera, F. Ronga, L. Satta, M. Spinetti, V. Valente; **Gran Sasso:** C. Gustavino, J. Reynoldson; **Indiana:** A. Habig, R. Heinz, L. Miller, S. Mufson, J. Musser, S. Nutter; **L'Aquila:** A. Di Credico, P. Monacelli; **Lecce:** P. Bernardini, G. Mancarella, D. Martello, O. Palamara, S. Petrera, P. Pistilli, A. Surdo; **Michigan:** E. Diehl, D. Levin, M. Longo, C. Smith, G. Tarlé; **Napoli:** M. Ambrosio, G. C. Barbarino, F. Guarino, G. Osteria; **Pisa:** A. Baldini, C. Bemporad, F. Cei, G. Giannini, M. Grassi, R. Pazzi; **Roma:** G. Auriemma, S. Bussino, C. Chiera, P. Chrysicopoulou, A. Corona, M. DeVincenzi, L. Foti, E. Lamanna, P. Lipari, G. Martellotti, G. Rosa, A. Sciubba, M. Severi; **Sandia Labs:** P. Green; **Texas A&M:** R. Webb; **Torino:** V. Bisi, P. Giubellino, A. Marzari Chiesa, M. Masera, M. Monteno, S. Parlati, L. Ramello, M. Sitta

*Univ. di Trieste

**Univ. della Basilicata

Although designed as a monopole detector, MACRO is also sensitive to "nuclearites" or strange quark matter in cosmic rays. The combination of a 3 month run in 1989 and a run from October 1989 to April 1991 has yielded a flux limit of $1.1 \times 10^{-14} \text{cm}^{-2} \text{sr}^{-1} \text{s}^{-1}$ for nuclearites with mass $10^{-11} \text{g} < m < 0.1 \text{g}$. For $m > 0.1 \text{g}$, the limit is $5.5 \times 10^{-15} \text{cm}^{-2} \text{sr}^{-1} \text{s}^{-1}$. The velocity range of nuclearites to which MACRO is sensitive extends down to near the escape velocity of the Earth and therefore covers almost all of the possible velocity range of nuclearites.

INTRODUCTION

The possible existence of an absolutely stable phase of quark matter, called strange matter or "nuclearites," has created much interest in the last few years.¹⁻⁵ Within the range of presently allowed QCD parameters, such strange matter may be the true ground state of QCD and may have a mass ranging from a few GeV to the mass of a neutron star. Since the possible mass of strange matter has such a wide range, its detection requires a variety of experimental techniques. These include mass spectrometer searches in terrestrial materials and analyses of natural disasters possibly caused by large pieces of strange matter hitting the Earth.^{3,4} Several cosmic ray searches have been carried out using scintillation detectors,^{6,7} ancient mica,⁸ plastic track etch detectors,⁹⁻¹¹ and a gravitational wave detector.¹²

MACRO (Monopole Astrophysics and Cosmic Ray Observatory) is an underground detector situated in Hall B of the Gran Sasso Laboratory in central Italy at an average depth of 3800 meter water equivalent.¹⁴ Although MACRO's primary physics goal is to search for magnetic monopoles, its monopole detection system will also detect charged cosmic ray strange quark matter that reaches the MACRO depth.

THE DETECTOR

The part of the MACRO detector used in this work, which is only 1/12 of the whole detector, consists of 10 horizontal layers of streamer tubes surrounded by two horizontal layers of scintillator counters on the top and bottom and three vertical walls of one scintillation layer and six layers of streamer tubes on the west, east and north sides. The dimensions of this part of the detector are 12 m long, 12 m wide and 4.8 m in height.

Two types of slow particle triggers were employed in this search. The first slow particle trigger (type I) is based on the time of passage of particles through a scintillator counter. This trigger system recognizes wide pulses or slow trains of single photoelectron pulses generated by slow particles and rejects large or short pulses caused by muons and radioactivity. The second slow particle trigger is based on the time of flight between walls and layers of scintillator counters. This system is simply a slow coincidence vetoed by a fast coincidence between them. When a slow particle trigger happens, the waveforms of both anode and dynode of the photomultiplier tubes (PMTs) are recorded separately by two waveform digitizers; each covers a different dynamical range.

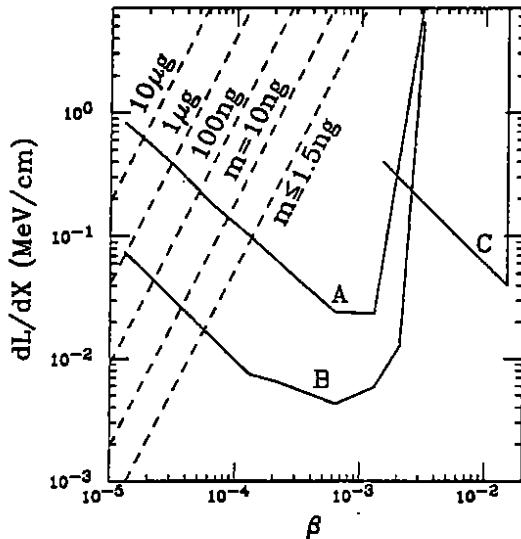


Fig. 1. Light yield of nuclearites in MACRO scintillator as a function of velocity ($\beta = v/c$) for different masses of nuclearites (dashes). The solid curves are the 90% trigger efficiency contours of MACRO slow particle trigger system. (A) Type I trigger based on time of passage in one scintillator counter before summer 1989; (B) The same Type I trigger after summer 1989; (C) Type II trigger based on the time of flight between scintillation counters.

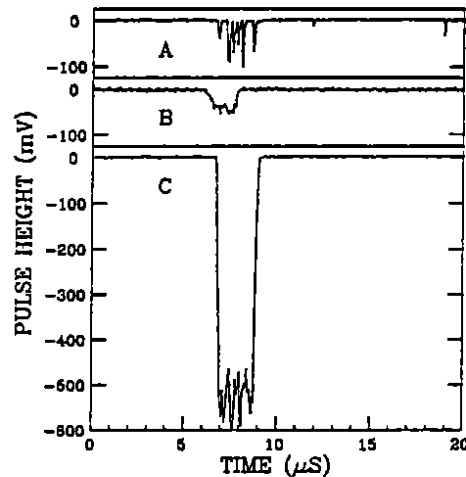


Fig. 2. (A): The waveform of the *best* slow particle candidate we found. (B): The waveform of an LED simulated event having roughly the same light yield as (A). (C): The Monte Carlo simulated waveform of a nuclearite with $\beta = 3 \times 10^{-4}$. All the waveforms are drawn in the same scale.

Fig. 1 shows the 90% trigger efficiency contours of our slow particle trigger system and lower limits of light yield of nuclearites for different masses. The 90% trigger efficiency contours are measured directly using simulated events obtained by driving LEDs with pulses of variable lengths and heights. The lower limit of the light yield of nuclearites is estimated from the blackbody radiation of the heated track³, including the blackbody radiation in the UV region which can be absorbed and re-emitted in the visible region¹⁴. Considerable improvements in the detector were made during summer 1989 and the slow particle trigger sensitivity increased by one order of magnitude, as shown in Fig. 1. The MACRO detector is sensitive to nuclearites as slow as $5 \times 10^{-5}c$, close to the escape velocity of the earth.

Muon triggers are also used in this search for fast nuclearites. When a muon trigger occurs, the pulse height and time of the PMT signals are recorded by ADCs and TDCs. Streamer tube hits are also recorded and then used to construct the muon track. Fast monopoles and strange matter can be recognized by their unusually high ionization yield.

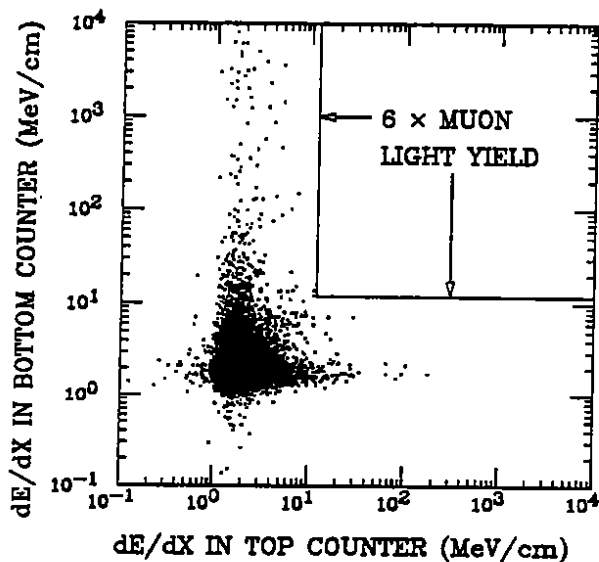


Fig. 3. Scatter plot of dE/dX in one wall versus dE/dX in another wall for muon events. There is no event having dE/dX in both walls greater than 6 times that of an ordinary muon.

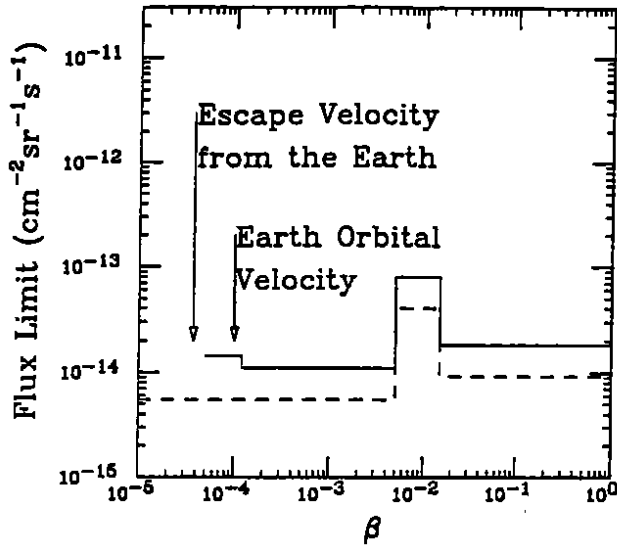


Fig. 4. Nuclearite flux limit as a function of $\beta = v/c$ from the combined MACRO searches. Solid line is for nuclearites smaller than 0.1g (not able to penetrate the Earth). The dashed line is for nuclearites that can penetrate the Earth (greater than 0.1g).

THE SEARCH AND THE RESULTS

In slow monopole searches, we required at least two scintillators to have triggers; this cut the data sample to only a few hundred events. Those events were then visually scanned to search for wide pulses or long pulse trains characteristic of a slow particle passing through the detector¹⁵. No such events with consistent light levels and photoelectron fluctuations were found. For the data set of Spring 1989, a search requiring only a single face trigger was also performed¹⁶ and this method increased the acceptance by about a factor of 2. Fig. 2 shows the waveform of the *best* slow particle candidate we found compared with the waveform of an LED simulated event and the Monte Carlo simulated waveform of a nuclearite with $\beta = 3 \times 10^{-4}$. All the waveforms are drawn in the same scale. The candidate waveform (A) shows a pulse train, but it is too spiky to be consistent with a slow particle. The waveform of a slow particle should look like waveform (B) which has about the same light level but is much smoother and has small fluctuations consistent with the photoelectron statistics. Furthermore, if waveform (A) were due to a nuclearite, its velocity would be $\beta = 3 \times 10^{-4}$ based on the length of the pulse train. At this velocity, however, a nuclearite should generate much more light and produce a waveform that would look like (C), quite different from waveform (A).

A fast monopole search was performed on our muon trigger data. In this search, we required consistency of streamer tube tracking and scintillator hits and then derived dE/dX in each scintillator counter after correcting for PMT saturation and light attenuation. The scatter plot of dE/dX in one scintillator wall versus dE/dX in another wall is shown in Fig. 3. A fast nuclearite ($\beta > 10^{-2}$) should have a dE/dX several orders of magnitude larger than that of a typical muon. As can be seen in Fig. 3, no event having a dE/dX in both walls greater than 6 times that of an ordinary muon was found.

The combined flux limits from all these searches are shown in Fig. 4 as a function of the nuclearite velocity. The MACRO search covers the velocity range from $\beta = 1$ down to $\beta = 5 \times 10^{-5}$. The MACRO limit, therefore, not only applies

to nuclearites of galactic or extra galactic origin but also applies to nuclearites that are trapped in our solar system.

REFERENCES

- ¹ E. Witten, *Phys. Rev. D* **30**, 272 (1984).
- ² E. Farhi and R.L. Jaffe, *Phys. Rev. D* **30**, 2379 (1984).
- ³ A. De Rujula and S. L. Glashow, *Nature* **312**, 734 (1984).
- ⁴ A. De Rujula, *Nucl. Phys. A* **434**, 605 (1985).
- ⁵ J. Madsen, H. Heiselberg and K. Riisager, *Phys. Rev. D* **34**, 2947 (1986).
- ⁶ K. Nakamura et al., *Phys. Lett.* **161B**, 417 (1985).
- ⁷ B. Barish, G. Liu and C. Lane, *Phys. Rev. D* **36**, 2641 (1987).
- ⁸ P. B. Price et al., *Phys. Rev. Lett.* **52**, 1265-1268 (1984).
- ⁹ K. Kinoshita and P. B. Price, *Phys. Rev. D* **24**, 1707 (1981).
- ¹⁰ P. B. Price, *Phys. Rev. D* **38**, 3813 (1988).
- ¹¹ S. Nakamura et al. UT-ICEPP-90-01 submitted to *Phys. Rev. Lett.*
- ¹² G. Liu and B. Barish, *Phys. Rev. Lett.* **61**, 271 (1988).
- ¹³ The MACRO Collaboration, *Nucl. Instr. Meth. A* **264**, 18 (1988).
- ¹⁴ The MACRO Collaboration, Proceedings of the Workshop on Strange Quark Matter in Physics and Astrophysics, Edited by J. Madsen and P. Haensel (to be published in Nuclear Physics B, Proceedings Supplements Section)
- ¹⁵ MACRO Collaboration, Proceedings of 21st ICRC, **10**, 75 (1990).
- ¹⁶ David J. Ficenec, Ph.D. Thesis, Boston University (1990).